Naval Research Laboratory

Washington, DC 20375-5320

NRL/MR/6180--07-9039

Intelligent Data Fusion for Wide-Area Assessment of UXO Contamination

SERDP Project MM-1510
2006 Annual Report

Susan L. Rose-Pehrsson
Kevin Johnson

Navy Technology Center for Safety and Survivability
Chemistry Division

Christian Minor

Nova Research, Inc.
Alexandria, VA

Verner Guthrie

U.S. Army Engineering Research and Development Center
Alexandria, VA

April 20, 2007

REPORT DOCUMENTATION PAGE

Form Approved
OMB No. 0704-0188

1. REPORT DATE *(DD-MM-YYYY)*	**2. REPORT TYPE**	**3. DATES COVERED** *(From - To)*
20-04-2007	Annual	December 2005 – November 2006

4. TITLE AND SUBTITLE

Intelligent Data Fusion for Wide-Area Assessment of UXO Contamination

SERDP Project MM1510
2006 Annual Report

5a. CONTRACT NUMBER
W74RDV53203308

5b. GRANT NUMBER

5c. PROGRAM ELEMENT NUMBER

6. AUTHOR(S)

Susan Rose-Pehrsson, Kevin Johnson, Christian Minor,* and Verner Guthrie**

5d. PROJECT NUMBER
SERDP Project MM-1510

5e. TASK NUMBER

5f. WORK UNIT NUMBER
61-9010-0-6

7. PERFORMING ORGANIZATION NAME(S) AND ADDRESS(ES)

Naval Research Laboratory, Code 6180
4555 Overlook Avenue, SW
Washington, DC 20375-5320

8. PERFORMING ORGANIZATION REPORT NUMBER

NRL/MR/6180--07-9039

9. SPONSORING / MONITORING AGENCY NAME(S) AND ADDRESS(ES)

Strategic Environmental Research and Development Program (SERDP)
Dr. Anne Andrews/Dr. Jeffrey Marqusee
901 N. Stuart Street, Suite 303
Arlington, VA 22203-1853

10. SPONSOR / MONITOR'S ACRONYM(S)

SERDP

11. SPONSOR / MONITOR'S REPORT NUMBER(S)

12. DISTRIBUTION / AVAILABILITY STATEMENT

Approved for public release; distribution is unlimited.

13. SUPPLEMENTARY NOTES

*Nova Research, Inc., 1900 Elkin Street, Suite 230, Alexandria, VA 22308
**U.S. Army Engineering Research and Development Center, Topographic Engineering Center, Alexandria, VA 22315

14. ABSTRACT

Intelligent data fusion techniques are being developed and optimized for use in enhancing wide-area assessment UXO remediation efforts. A data fusion framework will be created to provide a cohesive data management and decision-making utility that will capture all available data and more efficiently direct the expenditure of time, labor, and resources. The objectives of the first year are to determine the feasibility of feature selection methods for data fusion. The first year of project MM-1510 successfully demonstrated the feasibility of feature extraction from wide-area assessment survey data. In contrast to the individual data sources, feature extraction yielded enhanced data for the Pueblo PBR #2 that was well-suited for data fusion. Preliminary combination of feature maps from the various data sources yielded a map for the Pueblo site that was more accurate than any one data source alone. Probability densities were generated from the feature maps and make possible the combination of estimates of data quality, UXO-related features, non-UXO backgrounds, and correlations among the data sets in a Bayesian-based approach to data fusion.

15. SUBJECT TERMS

Data fusion; Wide-area assessment; Unexploded ordnance; UXO; Remediation; Data management; Decision-making utility; Feature selection methods; Probability densities; Bayesian-based; Wavelets; Principal component analysis; Image analysis

16. SECURITY CLASSIFICATION OF:			**17. LIMITATION OF ABSTRACT**	**18. NUMBER OF PAGES**	**19a. NAME OF RESPONSIBLE PERSON**
a. REPORT	**b. ABSTRACT**	**c. THIS PAGE**			Susan L. Rose-Pehrsson
Unclassified	Unclassified	Unclassified	UL	67	**19b. TELEPHONE NUMBER** *(include area code)* (202) 767-3138

Standard Form 298 (Rev. 8-98)
Prescribed by ANSI Std. Z39.18

Table of Contents

List of Acronyms

AMTADS	Airborne Multi-Sensor Towed Array Detection System
ASCII	American Standard Code for Information Interchange
CA	California
CO	Colorado
EMI	Electromagnetic Induction Magnetometry
ESRI	Environmental Systems Research Institute
ESTCP	Environmental Security Technology Certification Program
GDAL	Geospatial Data Abstraction Library
GeoTIFF	Geostationary Earth Orbit Tagged Image File Format
GIS	Geographic Information System
GPR	Ground Penetrating Radar
GPS	Global Positioning System
LiDAR	Light Detection And Ranging
MexGDAL	MATLAB program to interface with GDAL
MrSID	Multi-Resolution Seamless Image Database
NM	New Mexico
NRL	Naval Research Laboratory
nT	nanoTesla
PCA	Principal Components Analysis
PBR	Precision Bombing Range
RGB	Red-Green-Blue
SAR	Synthetic Aperture Radar
SERDP	Strategic Environmental Research and Development Program
TFM	Total Field Magnetometry
UTM	Universal Transverse Mercator Grid Coordinates
UXO	Unexploded Ordnance
WAA	Wide-Area Assessment
XYZ	Plain text data points provided as 2D coordinates and intensity

List of Figures

Acknowledgements

This research was supported wholly by the U.S. Department of Defense, through the Strategic Environmental Research and Development Program (SERDP). The authors thank the SERDP staff and team members for their assistance, particularly Dr. Herb Nelson and Dr. Dan Steinhurst.

Executive Summary

Background. The remediation of sites contaminated with unexploded ordnance (UXO) remains an area of intense focus for the Department of Defense. Current estimates place the total area of possibly UXO-contaminated sites at 10 million acres, with an overall cost of remediation with current methods and sensing technologies in the tens of billions of dollars. Fortunately, studies have estimated that up to 80% of typical sites of potential contamination are actually UXO-free. What is needed to take advantage of this ratio is a means to quickly and reliably scan large sites (on the order of 10,000 acres) in order to rapidly identify regions that are free of UXO and regions that must be subjected to more detailed and time-intensive examination and remediation with established UXO detection tools. Recent investigations have focused on wide-area assessments (WAA) aimed at rapidly determining the approximate density and spatial distribution of UXO objects over regions of wide area, rather than identification of individual UXO objects. Six wide-area assessment projects have been completed under the auspices of Strategic Environmental Research and Development Program (SERDP) and Environmental Security Technology Certification Program (ESTCP). [1] These projects utilized various detection techniques with different strengths and weaknesses. However, effective wide-area assessment has been hindered by a lack of accurate target and range information. In addition, no single sensing technology has been both accurate and cost-effective in surveying entire sites. Therefore, this project will work closely with the ESTCP Wide-Area Assessment Pilot Program to examine intelligent data fusion to improve detection and identification.

Objective. Intelligent data fusion techniques are being developed and optimized for use in enhancing wide-area assessment UXO remediation efforts. A data fusion framework will be created to provide a cohesive data management and decision making utility that will capture all available data and more efficiently direct the expenditure of time, labor and resources. In the first year of this project, the objectives are to determine the feasibility of feature selection methods for data fusion.

Methods. In the context of UXO remediation, intelligent data fusion is the combination of unbiased pattern recognition techniques with expert information about the strengths and weaknesses associated with the data acquisition techniques and expert knowledge of the geology, foliage, and man-made features located at the site under scrutiny. Data from multiple sensing modalities are utilized in an overall decision-making algorithm that is more accurate than any individual sensor on its own. [2,3] The data fusion algorithms are tailored to the data to extract the maximum information available from wide-area assessment sensing technologies. Sensor data are further leveraged by correlation with historical target and expert site information in the data fusion algorithms. In this manner, intelligent data fusion is able to augment the strengths of the different data types while minimizing their individual weaknesses to provide the most accurate wide-area assessment for the site given the available information.

To date, effective wide-area assessment has been hindered by a lack of accurate target and range information. In addition, no single sensing technology has been both accurate and cost-effective in surveying entire sites. The data fusion framework under

Manuscript approved March 5, 2007.

development in project MM-1510 is intended to bridge this performance gap and to do so in a manner that is as independent of the site data as possible, thus ensuring it is as widely applicable as possible. Therefore algorithm development is designed to emphasize methods for feature extraction, data fusion, and decision making that are general in nature and not overly site dependent. The data fusion framework will provide a set of algorithms and a process by which sensor data and auxiliary information can be combined to enhance ordnance-related signal and reduce false positives, independent of the specific sensor data and information available for any one site. The initial studies described in this report are focused on feature extraction and pattern recognition techniques that will provide input to the data fusion algorithms.

Results for Year One. Multiple wide-area surveys with different sensing technologies have been acquired under the ESTCP Wide-Area Assessment Pilot Program. The data resulting from wide-area surveys of the Pueblo Precision Bombing Range (PBR) #2 along with associated expert information regarding the site were used for this study. The Naval Reseach Laboratory (NRL) reviewed all the available data obtained from the ESTCP WAA Pilot Program survey of Pueblo PBR #2. This included magnetometry data acquired via helicopter survey (Helimag), LiDAR data in two resolution scales from airborne surveys, and orthophotography data from airborne surveys. Efforts at importing and registering data of various formats into the MATLAB environment were successful. Utilities for the importation of arbitrary geo-referenced image data and text data in XYZ format were also constructed and tested. In addition, a displacement of approximately four meters in geo-reference information was discovered in the orthophotography data acquired in 2004 relative to other survey data. SERDP and Skysearch were notified and this discrepancy was addressed and successfully rectified.

NRL obtained and reviewed auxiliary information for the Pueblo PBR #2. This expert information was comprised of topological maps, geological survey data, and the archive search report for the site. Historical usage indicated a training range with a bombing camp and nine precision bombing targets. Anecdotal information in the archive search report also indicated the presence of a suspected 75 mm air-to-ground target and pattern gunnery range. These data were utilized to generate a historical target feature map of likely UXO contamination. Geological survey data indicated that the Pueblo site contained minimal magnetic geological features. Foliage and other ground surface features that may interfere with data acquisition were also minimal at the site. Such features are expected to significantly affect data acquisition and quality at other sites, and therefore will be incorporated into feature maps where relevant.

NRL evaluated the current state-of-the-art in data analysis and data fusion algorithms for the sensing technologies employed in the ESTCP WAA Pilot Program surveys. A literature review indicated that the current state-of-the-art was generally focused on algorithm development for the detection of specific objects, and was therefore more suitable for local area applications than for wide-area assessment. Algorithms for orthophotography data emphasized classification of ground cover type through texture analyses or pattern recognition. Though the Pueblo site lacked significant ground cover, these algorithms may be applied to orthographic data from other surveyed sites. For

LiDAR, algorithms were specific to the applications, which were mostly environmental. However, the general approach used for algorithm development proved useful in feature analysis. For magnetometry data, algorithms focused on physical modeling as a method of the detection of individual objects and required sensitivities not attainable in helimag surveys. Approaches to data fusion typically applied multivariate analysis to time and/or frequency domain EMI data to distinguish individual objects as well. EMI is a data source not yet available for wide-area assessment.

NRL performed feature selection specific to each data source to optimize the extraction of information relevant for wide-area assessment. As part of this effort, NRL also developed and implemented pattern recognition algorithms for all selected features in the sensor data obtained from the ESTCP WAA Pilot Program surveys. Methods for feature maps suitable for auxiliary information were discussed above. Craters were the principal UXO-related feature of the LiDAR and orthophotography data, and total magnetic content for the magnetometry data. For the LiDAR and orthophotography data, the main components of the backgrounds to feature selection were geology, foliage, and man-made structures. For the magnetometry data, geology and man-made structures contributed to the background while foliage was not a significant factor.

Of the three survey data sets, the orthographic data were the least informative source for the Pueblo PBR #2. Extraction of craters was not nearly as efficient as with the LiDAR data, and the minimal presence of foliage and man-made structures at this site made positive identification challenging. Thus, autonomic pattern recognition yielded features with very low signal-to-noise ratios. Crater extraction from the LiDAR data was successful. An algorithm based on the circular Hough transform was able to extract a value of four meters as the characteristic diameter of craters at the Pueblo site. Further, a pattern recognition algorithm based on the morphology of the craters was developed to locate them in the LiDAR data. This information was then converted into a feature map describing the density aspect of craters. Feature maps describing the intensity and quality aspects to craters may also provide data fusion algorithms with additional discriminatory information.

Feature selection was most successful with the magnetometry data. The total magnetic signal approach quickly yielded a feature map that displayed all relevant ferromagnetic signals from ordnance-related material and man-made structures present in the data from the surveyed area of the Pueblo PBR #2. Due to the minimal geomagnetic features at the Pueblo site, a simple threshold proved effective in eliminating geologic background, which is expected to be more significant at other ESTCP WAA Pilot Program sites. A pattern recognition algorithm was developed to separate ordnance-related signal from the ferromagnetic background of man-made structures. This information was then converted to a feature map describing the density aspect of ordnance-related material. Separate feature maps describing the intensity and morphology aspects of the ordnance-related and man-made components of data are also expected to provide additional discriminatory information for data fusion.

NRL developed a multi-resolution algorithm for converting feature maps to probability densities, which are required for the proposed Bayesian-based approach to data fusion. The multi-resolution algorithm used a computationally-intensive approach similar to that of Parzen windows. [5] The generation of probability densities is a key enabling component for data fusion work slated for year two.

NRL also explored methods and algorithms for locating feature correlations among the various data sources. Visual inspection of data from the three surveyed sources revealed apparent spatial collocation of crater and ferromagnetic features. To quantify these correlations, principal components analysis (PCA) was applied to the data sets simultaneously. The application of PCA resulted in no useful information as the features were too obstructed by background. However, comparison of the crater and magnetometry feature maps for the southern portion of the Pueblo site to the combined feature map indicated that the features were not exactly spatially correlated. The incidence of cratering was most dense in the region between the two peaks of ordnance-related magnetic signal. Therefore, algorithms to quantify feature correlations from data subsequent to feature extraction will be developed in the second year of the project.

First year efforts for feature extraction were successful. Features relevant for wide-area assessment of UXO contamination were successfully obtained from the various data sources. Taken individually, the results for each data source (expert information, orthophotography, LiDAR, and magnetometry) did not provide an accurate wide-area assessment of the Pueblo site. However, when the results were considered in tandem the extracted features provided a more accurate wide-area assessment of the Pueblo site. For example, the crater-like feature density map filled in the gap between the two peaks in the southern portion of the magnetometer signal density map. Thus, the target range known to be present in this area was used more extensively than indicated by historical sources. In addition, the density maps and the combined map all confirmed the presence of a second, but less used, target range located in the northern portion of the Pueblo site. No evidence in these maps supports the existence of the suspected 75 mm range. Ground truth dug in all three of these regions affirmed these conclusions.

Conclusions: The first year of project MM-1510 successfully demonstrated the feasibility of feature extraction from wide-area assessment survey data. In contrast to the individual data sources, feature extraction yielded enhanced data for the Pueblo PBR #2 that was well-suited for data fusion. Preliminary combination of feature maps from the various data sources yielded a map for the Pueblo site that was more accurate than any one data source alone. Probability densities were generated from the feature maps and make possible the combination of estimates of data quality, UXO-related features, non-UXO backgrounds, and correlations among the data sets in a Bayesian-based approach to data fusion.

The feature extraction algorithms and the tiered approach to data fusion developed in the first year will enable a data fusion framework for wide-area assessment to be an effective tool for UXO remediation of other sites. Although tailored to the specific data sources, the algorithms developed are general in nature and not overly site dependent. Large

variations in the backgrounds for extracted features are expected for different remediation sites. However, these variations will most affect the signal-to-noise ratios in the maps of extracted features. The strength of a data fusion approach is that it provides resilience to such variations by maximizing the information obtained from the different data sources and minimizing exposure to false positives and background variations. The methods will provide a means to develop additional feature maps to quantify specific background features. Thus, the feature extraction algorithms and tiered approach to data fusion will be applicable to data sets from other survey sites. In summary, the results from the first year of project MM-1510 have only strengthened the case for the effectiveness of a data fusion approach for wide-area assessment.

Benefits. Key advantages of systems based on data fusion are the ability to reduce false positives while retaining high detection rates and the inherent flexibility of Bayesian decision trees. Such a framework utilizes the information it has available, without necessarily requiring that the exact same inputs be present at each application. This flexibility is an important feature of the data fusion approach as it is expected that, for a number of reasons, it will rarely be the case that exactly the same types of data will be available for analysis each time a wide-area UXO assessment is performed. Previous work at NRL has demonstrated the success of such techniques in simultaneously improving detection and reducing false positives in shipboard damage control system architectures based around multiple sensor inputs. It is expected that these benefits will be realized in UXO detection applications as well. Additional benefits that will follow from this research are a better understanding of the relationships between different sensor technologies, the impact of these relationships on overall efficacy at UXO detection, and ultimately, the knowledge to help design more efficient UXO surveys in the future.

Future Applications. MATLAB was chosen as the computational platform for initial algorithms. As a research tool, MATLAB provides an extensive code base, with the ability to port MATLAB implementations to other computational platforms following development. It is expected that MATLAB will not be utilized as a production platform to implement the data fusion framework for use by site administrators. Rather, a solution that involves partnering with an existing GIS software vendor would be preferable. In the final year, we will meet vendors suggested by SERDP program managers to develop a detailed plan for transitioning the data fusion framework to a platform suitable for onsite implementations. As part of this effort, we plan to demonstrate the capabilities of the data fusion framework at an appropriate site.

Objective

The objective of project MM-1510 is to enhance assessment of buried unexploded ordnance (UXO) in large geographic areas through data fusion of outputs of multiple sensing technologies with any available expert knowledge of the sites. The result of an intelligent combination of data feature analysis and site information will be wide-area maps of potentially contaminated sites delineating areas of likely UXO contamination from those that are free of UXO. Such maps show density of ordnance-related material, which is related to a likelihood of UXO contamination. These assessments will then direct the acquisition of data using more accurate, sensitive, and costly local-area UXO surveys. Data from local-area surveys can then be fed back into the data fusion framework and used to further refine maps of these regions and to provide more detailed assessments.

Project MM-1510 centers on the development and demonstration of a cohesive data management and decision making utility for enhancing UXO survey efforts. This will be accomplished by providing an algorithmic means of utilizing complementary information from multiple sensing technologies corroborated with expert site information to reduce overall false alarm rates and thus enhance wide-area UXO assessment efforts. A tiered approach to UXO assessment is being developed in which data from the wide-area sensing technologies are first processed by data fusion algorithms. The resulting output is then used to help direct progressively more local and time intensive efforts where they are most needed. The process as a whole is called the "data fusion framework" and will benefit site remediation by allowing more efficient direction of time, labor, and resources.

This report describes the first year of a three-year effort to develop the data fusion framework. The first year objectives were to determine the feasibility of feature extraction methods to provide complementary data from the various detection sources that will be used in intelligent data fusion.

Background

Problem Statement

Current estimates place the total area of possibly UXO-contaminated sites at 10 million acres, with an overall cost of remediation with current methods and sensing technologies in the tens of billions of dollars. Studies have estimated that up to 80% of typical sites of potential contamination are actually UXO-free, indicating a need to quickly and reliably scan large sites (on the order of 10,000 acres) in order to rapidly identify regions that are free of UXO and regions that must be subjected to more detailed and time-intensive examination and remediation with established UXO detection tools.

Effective wide-area UXO assessment is centered on the capability to rapidly scan large tracts of land and obtain relevant, useful information in the process. Two possible modes

of enhancement to wide-area UXO assessment are, first, decreasing the false alarm rate of current UXO sensing technologies, and second, utilizing alternate sensing technologies and survey methods that scan larger areas or more rapidly cover large areas than current sensing platforms.

Current Technology

Standard, ground-based UXO sensing technologies include methods such as vehicular-mounted time and frequency domain electromagnetic induction (EMI), total field magnetometry (TFM), and ground penetrating radar (GPR).[*] These UXO sensors have been deployed on ground-based platforms such as portable devices, push carts, and towed sensor arrays. Standard analysis methods of these types of data are well described in the literature and have been implemented with success. These methods typically rely on generating theoretical sensor response models, or measuring pure responses of various UXO items and then comparing survey data to these models in order to make a detection or classification. Typically, the ability of such techniques to cover wide survey areas is limited, although current SERDP projects are assessing the utility of ground survey transects to increase this capability for wide-area applications.

It is expected that any sensing technology suitable for WAA will have to be deployed from fixed wing aircraft, some other airborne platform such as helicopters, or even high-altitude surveillance such as high-resolution satellite imagery in order to rapidly scan larger areas. Such sensing will necessarily be remote relative to current methods for detection and classification of individual UXO objects, and that new sensing methods and data analysis technologies may be more applicable. Thus, increasing the area scanned is likely to require both new sensing technology and new sensor deployment platforms.

Demonstrated potential wide-area UXO sensing technologies fall into four broad groups: electromagnetic sensing, ground-penetrating radar and visible light imaging, thermal imaging, and hyperspectral imaging, all of which generate data in the form of maps (i.e. images, sometimes with additional depth information) that are spatially correlated with Global Positioning System (GPS) data or some other geo-referencing tool. [1] Of these, electromagnetic sensors are the most widely researched and deployed technology for the task of detection of buried UXO. The Naval Research Laboratory's Airborne Multi-Sensor Towed Array Detection System (AMTADS) is capable of scanning 500 acres per day, flying at a height of three meters. However, at distances greater than three meters individual UXO objects rapidly become lost among the signals due to geological features; a consequence of signal strength on the cube-root of distance. Nonetheless, application of magnetometry is proving to be useful for wide-area assessment.

As the sensitivity/ ground penetration depth of direct UXO sensing technologies drops steeply with distance, alternate techniques for wide-area assessment will generally not have the benefit of sensing deeply buried UXO objects directly. Instead, they must rely

[*] See "*Proceedings of SPIE:* Detection and Remediation Technologies for Mines and Minelike Targets V through VIII" and "*Transactions on Geoscience and Remote Sensing, Vol 2, No. 3, (2001)*" for examples.

instead on sensing UXO-related phenomena like spectral chemical signatures, variations in heat capacity, and measurements of surface clutter and micro-topological features. The techniques of synthetic aperture radar (SAR), light detection and ranging (LiDAR), and high-resolution aerial photography all yield information about micro-topological features and surface clutter of wide areas under assessment. These sensors have the benefit of functioning over much greater distances than electromagnetic sensors, allowing them to be deployed on fixed wing aircraft. With this group of sensors, the primary mode of detection relies on the location of micro-topological features associated with UXO, such as craters, infrastructure remnants, rather than the direct detection of individual UXO objects. Thermal imaging techniques yield information about variations in heat capacity across large areas and such images have been shown to be useful in location of UXO by sensing associated anomalies in heat capacity. Finally, hyperspectral imaging techniques yield information regarding the chemical composition of wide areas of soil that can potentially be used to detect the presence and concentration of UXO. Towards this end, six wide-area assessment projects have been completed under the auspices of SERDP and ESTCP. [1] These projects utilized techniques that varied from airborne infrared laser imaging combined with thermal imaging (UX-9523), synthetic aperture radar (UX-0126, UX-1070, and UX-1173), and airborne magnetometer arrays (UX-0031 and UX-3002).

Data Fusion Approach

To date, effective wide-area assessment has been hindered by a lack of accurate target and range information. In addition, no single sensing technology has been both accurate and cost-effective in surveying entire sites. The data fusion framework under development in project MM-1510 is intended to bridge this performance gap and to do so in a manner that is as independent of the site data as possible, thus ensuring it is as widely applicable as possible. The algorithm development is therefore designed to emphasize methods for feature extraction, data fusion, and decision-making that are general in nature. The data fusion framework will provide a set of algorithms and a process by which sensor data and auxiliary information can be combined to enhance ordnance-related signal and reduce false positives, independent of the specific sensor data and information available for any one site.

As has been discussed, there are two primary modes by which wide-area UXO assessment capabilities can be enhanced. First, the high false alarm rate of current UXO sensing technologies could be reduced, resulting in a reduction of time spent excavating non-UXO objects and allowing greater land coverage in a given period of time. Second, alternate sensing technologies and survey schemes could be employed to increase data throughput/ land coverage in a given period of time. The data fusion approach under investigation in project MM-1510 is directly aimed at both of these modes of enhancement.

In the context of UXO remediation, intelligent data fusion is the combination of unbiased pattern recognition techniques with expert information about the strengths and weaknesses associated with the data acquisition techniques and expert knowledge of the

geology, foliage, and man-made features located at the site under scrutiny. Data from multiple sensing modalities are utilized in an overall decision-making algorithm that is more accurate than any individual sensor on its own. [2,3] The data fusion algorithms are tailored to the data to extract the maximum information available from wide-area assessment sensing technologies. Sensor data are further leveraged by correlation with historical target and expert site information in the data fusion algorithms. In this manner, intelligent data fusion is able to augment the strengths of the different data types while minimizing their individual weaknesses to provide the most accurate wide-area assessment for the site given the available information.

Figure 1 breaks down the proposed data fusion framework into five steps for wide-area assessment of an individual site. The first step is the acquisition of all available sensor data and auxiliary site information. A common, uniform grid for the site that encompasses all surveyed areas is generated from a preliminary examination of the data. Locations on the common grid serve as indexes for database storage of sensor and site information pertinent to that grid location. The second step is the registration of sensor data and site information to the common grid and their incorporation into an easily accessible database format. As part of the registration process, data are analyzed and data quality metrics are established, if possible. Signals may be interpolated to fill gaps between data caused by geological impediments or from widely spaced "transects" in wide-area scans.

The engine of the data fusion framework is in the third step, where data enhancement, data fusion, and algorithmic processing are performed. Acquired sensor data are processed according to standard analysis algorithms as well as with additional feature selection algorithms specifically developed for each sensing technology. Processed sensor data and relevant auxiliary information are then combined with Bayesian-based data fusion algorithms to uncover correlations and establish confidence levels for locations on the grid. These algorithms are "smart" in that they incorporate into their calculations the strengths and weaknesses of the various sensor data and pieces of auxiliary information. Finally, the data fusion results are analyzed via a Bayesian decision tree that examines grid locations across multiple size scales and then calculates preliminary UXO probabilities for the surveyed area.

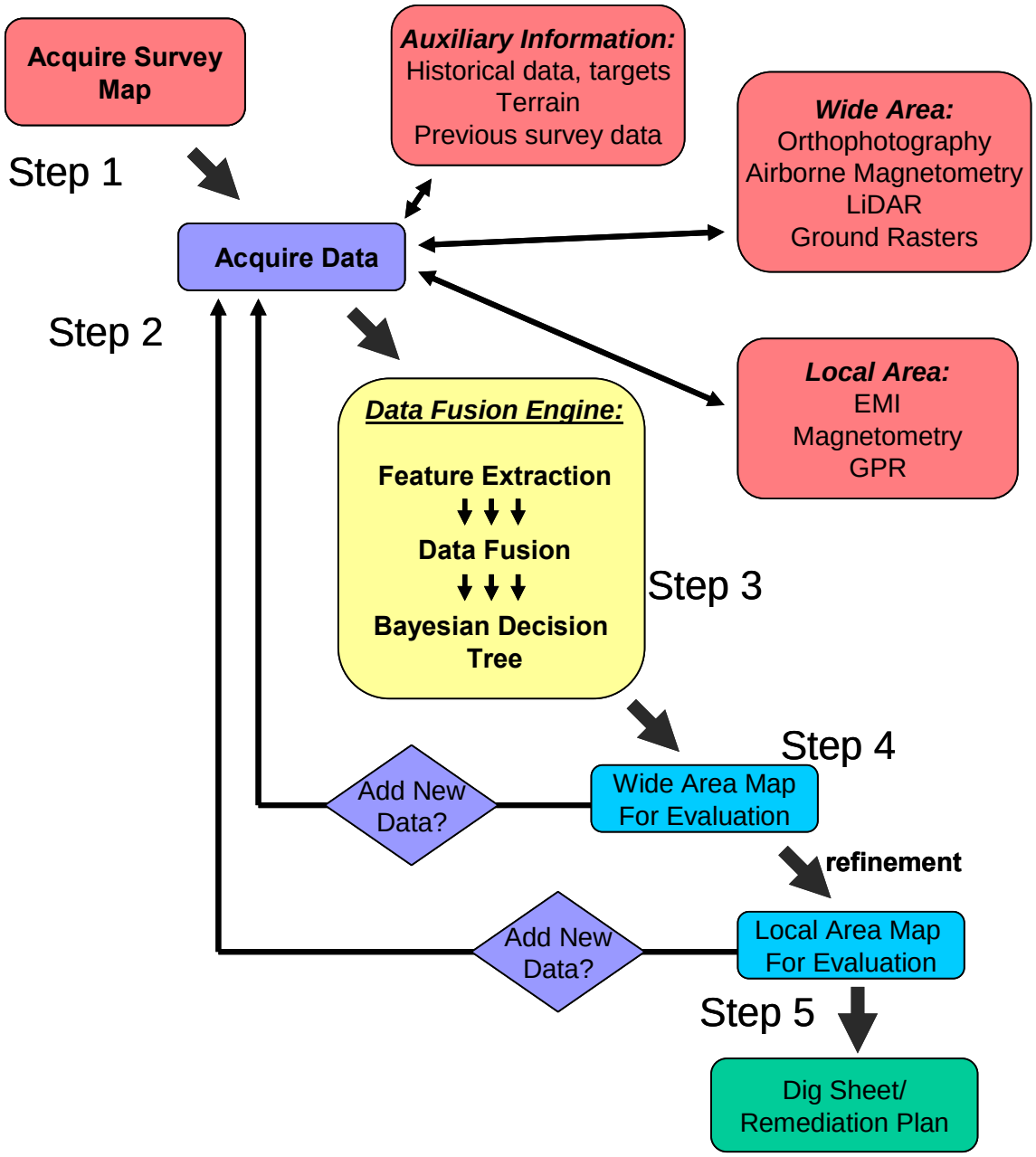

Figure 1 Implementation of a data fusion framework for wide-area UXO assessment

In the fourth step, the output of the decision tree is assimilated into a wide-area assessment map of the surveyed area. Points on the map are scaled and color coded by likelihood to indicate the density of ordnance-related material. In step five, regions of the wide-area assessment map delineating areas with a high probability of UXO contamination can be refined and enhanced with additional survey scans that acquire more detailed data. Data from these more sensitive and higher resolution scans of contaminated areas can then be fed back into the data fusion framework, refining UXO probabilities towards an accurate local area assessment and dig sheet. One advantage of the data fusion framework is that new data can be processed and incorporated into the

WAA map or the refined local area maps as it becomes available. This sequence (steps 2 – 5) is repeated until UXO contamination is acceptably mapped for the survey area. Remediation efforts are directed by a map-based display of UXO locations/classifications output by the Bayesian decision tree utilized by the data fusion framework.

The data fusion framework is based on a tiered approach to data analysis, described in steps 1 – 3 above. Each successive tier of analysis builds on the results obtained in lower tiers by examining the data in an expanding context of new features and auxiliary information. The development of methods for each tier proceeds as follows:

First, data are acquired and registered to a common, uniform grid using standard interpolation and averaging techniques where needed. Data quality metrics are used to quantify any adjustments made to data and also serve as a numerical confidence measure for data at individual locations on the grid. Historical target, relevant geological data, and other auxiliary information are also registered to the common grid. Next, registered sensor data are processed with standard signal processing tools and subjected to exploratory feature selection algorithms to identify UXO-relevant features. In parallel with this, the space of available dataset and feature combinations is examined to identify useful correlations across sensor platforms and prune redundant information. Computationally-tractable pattern recognition techniques for selected features are then developed and implemented. The density, intensity, and morphology of features and correlations are quantified as probability densities for all locations on the grid.

Next, a set of data fusion algorithms to combine feature maps and auxiliary information are developed by applying empirical and theoretically guided heuristics to choose appropriate decision and data combination rules. The development of data fusion algorithms is guided and measured by their ability to enhance ordnance-related signal and reduce false positives in the context of available data and information. Finally, a Bayesian decision tree is developed to examine and assess the results obtained from prior analyses on multiple size scales in a statistically rigorous manner. The use of a Bayesian approach for the decision tree provides resilience to missing or corrupted data, and resilience to imperfect feature classifications and auxiliary information. Note that the development process is by design not dependent on any specific type of sensor data or auxiliary information. Data from new sensing technologies and site information can therefore be incorporated into the data fusion framework for a site as they are developed and analyzed.

Development, implementation, and evaluation of project MM-1510 has been planned on a three-year schedule. In the first year, the principle tasks are to extract features relevant for data fusion from the sensor data and to determine the feasibility of feature extraction to enhance ordnance-related signal and reduce false positives. In the second year, data fusion algorithms and the Bayesian decision tree will be developed and evaluated. In the third year, the data fusion framework will be optimized and demonstrated.

Methods

The overall goal for the first year of project MM1510 was to demonstrate the feasibility of feature extraction from wide-area assessment survey data to enhance ordnance-related signal and to reduce false positives when used as input to data fusion. Successful application of data fusion requires two characteristics for input data sets. First, no single data source can cost-effectively provide the required information on its own, and second, the available data sources must be complementary, providing additional information not present in the other sources. Without the first characteristic, there is no need for data fusion; without the second characteristic, there is no benefit from data fusion. Thus, first year efforts were directed towards elucidating complementary features from the various detection methods, geologic data, and historical site information. An assessment of extracted features will serve as the basis for a go/no go decision for continuing the project into the second year: data fusion framework development. The completed first year components of the data fusion framework are illustrated in Figure 2.

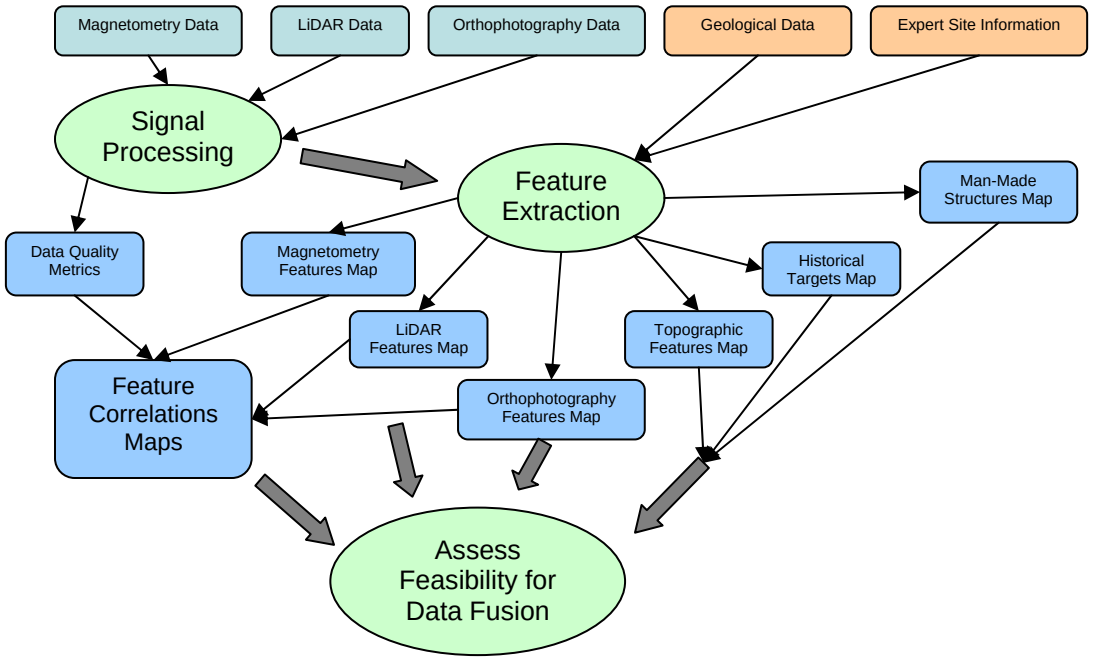

Figure 2 Diagram of completed first year components of the data fusion framework.

The first step was to obtain wide-area UXO survey data from the ESTCP Wide-Area Assessment Pilot Program. Next, a review of sensor data and acquisition algorithms was performed in order to assess the feasibility of incorporating current data metrics into a potential data fusion framework. Concurrently, available auxiliary information was reviewed for the selected site. Features determined to be useful for UXO assessment were identified in the available data sets. Finally, work was performed to develop custom

pattern recognition and feature extraction algorithms based on our sensor data and data algorithm review.

Sensor Data Review

The first step was the acquisition of data for feature selection and algorithm development. This work leveraged data that were acquired by SERDP/ESTCP programs, specifically, data acquired during the ESTCP Wide-Area Assessment Pilot Program. The WAA Pilot Program examined three former Department of Defense sites in 2004 and 2005. The three sites surveyed were: Pueblo Precision Bombing Range #2 in Colorado (CO), Former Kirtland Bombing Targets N1 and N3 in New Mexico (NM), and the Military Wash Area in the Borrego Maneuver Area in California (CA). The principle sensing modalities utilized in each survey were low altitude (helicopter) airborne magnetometry often referred to as Helimag and high-altitude airborne LiDAR and orthophotography.

The next step was the conversion and registration of data sources to a common grid and format. MATLAB [4] was chosen as the computational platform for initial algorithm prototyping, and this choice dictated the data format. MATLAB provides an extensive code base, and the ability to port MATLAB implementations to other computational platforms following development. It is expected that MATLAB will not be utilized as a production platform for this work. For production code, a solution that involves partnering with an existing GIS software vendor would be preferable for several reasons.

Two grid spacings were selected for feature development, half meter and one meter. It is possible to develop features in the native space of the data and then register the features to a common grid. However, this approach was not taken as it does not allow for an examination of the impact of data resolution on feature extraction, which may be relevant to data acquisition costs.

Expert Information Review

As part of the Wide-Area Assessment Pilot Program discussed earlier, ground truth data were to be obtained for each site. Information of this type is useful for assessing the utility of auxiliary data, the accuracy of feature extraction from sensor data, and, ultimately, for evaluating the probabilistic output the data fusion framework. Thus, all available ground truth data were obtained for inclusion in feature development.

Aside from ground truth data, auxiliary information regarding potential UXO contamination at a perspective UXO survey site was acquired to assess its potential to enhance data fusion. Archive search reports for each site consisting of items such as historical records of site usage, data from previous surveys, first hand experience of local inhabitants, and other sources of expert knowledge were also obtained for review. The inclusion of this additional information is expected to be useful in regions where geological features and surface phenomena inhibit or alter sensing technology results.

Evaluation of Current Sensor Algorithms

A literature survey was performed in order to research current UXO data analysis strategies and to assess their utility for extracting features for data fusion. Software packages commonly used in the evaluation of UXO data were obtained and evaluated for their ability to efficiently process large data streams, to locate features relevant for wide-area assessment, and to export such information to the development platform. Data provided in multiple, algorithmically-altered forms were evaluated to determine the impact of the alterations to subsequent feature analyses and data fusion.

Feature Selection to Optimize Information and Pattern Recognition Implementation

The feature selection and pattern recognition tasks are closely linked. The investigations focused on locating features relevant to UXO assessment within the wide-area assessment data gathered, and also on determining what types of signal processing algorithms would be useful in extracting those features in an automatic fashion. The extracted feature sets will ultimately form the inputs into any potential data fusion algorithm. Utilizing expert information and ground truth regarding the survey site, regions of interest were located. Data features exhibiting a causal or correlative link with UXO-related items were flagged and examined as well as features associated with the absence of UXO-related items. The utility of various data analysis techniques was evaluated for potential in automatic extraction of these features, or otherwise marking regions associated with known UXO contamination. The acquired raw and processed sensor data were also examined to evaluate the ability of external signal processing techniques to remove redundancies and to identify previously unseen correlations and features in and between the data sets.

The approach to feature analysis was based upon examining three aspects of identified features, their density, intensity, and morphology. The density aspect of identified features quantified the number of features identified per unit survey area, irrespective of feature strength or shape. The intensity aspect of features quantified their strength, and the morphology aspect quantified their shape. These feature aspects were used to construct probability density maps that described the density, intensity, and morphology aspects of the features, or combinations thereof. Such maps are well-suited to a Bayesian approach to data fusion. Probability density was calculated via successive approximations of aspect density (i.e., probability mass) in local regions of decreasing size, as in the Parzen window approach.[5] The goal was to find features whose probability density maps correlated (or anti-correlated) with UXO contamination as identified with auxiliary information and human review of the survey data. For a variety of reasons, it was not expected that, on a feature by feature basis, all three of these aspects would necessarily prove to be simultaneously useful to achieving this goal.

The final task of the first year of project MM1510 was to implement the feature selection techniques deemed to have utility in extracting UXO-relevant features from wide-area survey data. The last criterion for feature utility was that its extraction from survey data

be performed with reasonable computational resources. Development efforts focused on finding computationally-tractable methods of executing the feature extraction algorithms on very large data sets, and determining optimum parameters for algorithm usage.

Results and Accomplishments

Sensor Data review

Part of the ESTCP Wide-Area Assessment Pilot Program was assigned for use in feature extraction development and in training data fusion algorithms. This subset included the data resulting from wide-area surveys of the Pueblo Precision Bombing Range #2 (CO) and half of the data from Former Kirtland Bombing Targets N1 and N3 (Kirtland AFB, NM). The remaining half of the Kirtland site and all of the Military Wash Area in the Borrego Maneuver Area (Victorville, CA) site were reserved for blind testing of the resultant data fusion framework. The studies described here used all the Pueblo site survey data files and associated information.

The survey data obtained for the Pueblo site consisted of image files containing aerial LiDAR and orthophotographic surveys, and a series of text files containing data from a low-altitude (helicopter) survey. The aerial LiDAR survey of the Pueblo site was received as two Environmental Systems Research Institute (ESRI) "*.adf" files (arc/info binary file format). One file comprised a square region in the southwest corner of the survey region that had been acquired in 2004. The other file comprised the remaining area of the survey and had been acquired in 2005. Within these files, image pixel values were represented as 32-bit floating point numbers. Images were recorded at 0.4m resolution in the first file and at 0.5m resolution in the second. The aerial orthophoto survey of the Pueblo site was received as two Multi-Resolution Seamless Image Database (MrSID) "*.sid" files. These surveys were acquired concurrently with the LiDAR survey and comprised the same areas of the survey region. Each image was recorded at a resolution of 0.139m and each pixel's value was represented by three 8-bit integers representing red, green, and blue intensities. The magnetometry survey of the Pueblo site was received as a series of ten ASCII text files containing six columns of information representing Zone 13 UTM Northing and Easting coordinates, magnetometer reading, height above ground, height above ellipsoid, and time of acquisition.

The first step in the review of the acquired data was to import the data into the MATLAB computational environment for viewing and further analyses. A suite of MATLAB routines was assembled to provide a turn-key approach to importing the image and XYZ format data into the MATLAB workspace environment. This accomplishment allows for convenient and rapid access to all survey data from within the MATLAB workspace, and makes possible the rapid importation of new survey site data in the future. The critical functions that these routines perform are as follows:

1. Accepting user input of coordinates specifying a rectangular region within which the survey site lies that serves as a common geospatial grid of user specified resolution upon which multiple survey results and algorithm outputs are projected.
2. Dividing the common grid region into user-specified square subsets, called "blocks," to allow for analysis of local regions without requiring the retrieval of data from the entire survey site.
3. Importation of geo-referenced imagery into the MATLAB computational environment, and utilizing interpolation or down sampling to register it to the common grid.
4. Importation of so-called "XYZ" format data points such as those received from the helicopter magnetometry survey to the common grid.
5. Wrapping all survey data and associated metadata (UTM coordinates, description of data layers, etc.) into a single data structure (i.e., database) for each subset block of the common grid.

In order to import geo-referenced image data into MATLAB, the geospatial data abstraction library (GDAL) was obtained and installed along with the MATLAB "mexGDAL" toolbox [6], which provides an interface between the GDAL library[7]and MATLAB. Due to the proprietary nature of the original image file formats, the image data files were first converted into geo-referenced images in "GeoTIFF" format and then imported into MATLAB.

The conversion of magnetometer survey data into continuous surface estimates required the following steps. For each subset block of the common grid, the magnetometer data text files were automatically searched for data points whose UTM coordinates fell within the geo-referenced boundaries of that subset block. These points were read into MATLAB as double precision floating point numbers. Next, the data points falling within a square around a location on the grid (i.e., pixel) were averaged. The size of these grid pixels was specified by the resolution of the common grid. Following averaging, the values of pixels for which no data points were located were estimated via interpolation based on the values of neighboring points. Lastly, data quality metrics of data point density and variance for each pixel on the common grid surface were calculated for diagnostic purposes and for potential inclusion in future data fusion algorithms. These data quality metrics are depicted in Figure 3(a) and (b).

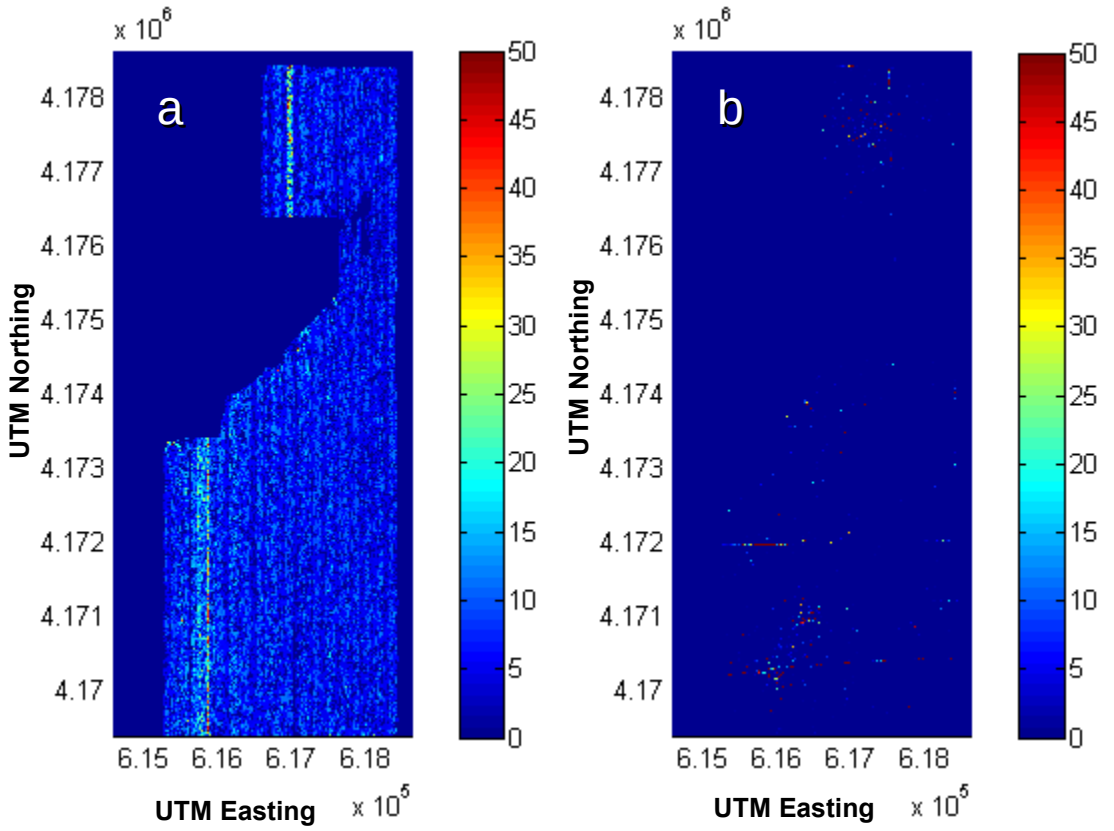

Figure 3 Magnetometer signal data quality metrics: (a) data point density and (b) variance per image pixel.

For the Pueblo Precision Bombing range area, the common grid was specified based on an examination of the furthest extents of each of the different survey data sets. This grid spanned the range between UTM Northing 4,169,390 to 4,178,634 and UTM Easting 614,590 to 618,627, (Zone 13) and represented a rectangular survey area of approximately 37 square kilometers. This grid was then divided into regularly sized blocks that were 1024 meters to a side, starting at the SW corner and moving south to north and west to east. For each block, the appropriate data were loaded from the source file and interpolated to fit a 1m or 0.5m resolution grid. The data were saved on a block by block basis in a MATLAB database where each data layer occupied a different field in the structure. Thus, correctly registered, survey-wide data were made available for subsequent feature extraction and processing.

Note that the survey area of the Pueblo site represented roughly 40 million pixels of information at one meter resolution, or, roughly 4 gigabytes of information. For comparison, the memory available in a typical modern desk-top computer is 1 gigabyte; in that of scientific workstation, 4 gigabytes. As a consequence, an emphasis on maintaining computationally-tractable methods for data analysis was a necessity for algorithm development.

Expert Information Review

The archive search report and available US geological survey information for the Pueblo PBR #2 site [8] were obtained and reviewed. A detailed topological map showing man-made and natural features within the Pueblo site was obtained for visualization and analysis purposes and registered to the common grid along with the WAA survey data.

The former Pueblo Precision Bombing and Pattern Gunnery range #2 is in Otero County, Colorado and is characterized by flat to rolling hills covered with grass and low bushes. Figure 4 shows the portion of the Pueblo site that was surveyed with imagery. Figure 5 shows a photo of the terrain. [9] The range is approximately 20 miles south of La Junta, Colorado. The area was used for cattle grazing until the War Department assumed control of the lands for a period spanning 1942 to 1945. Currently, the lands are primarily managed by the U.S. Forest Service as the Comanche National Grasslands with some portions leased to private owners for grazing or else owned by the State of Colorado. [10]

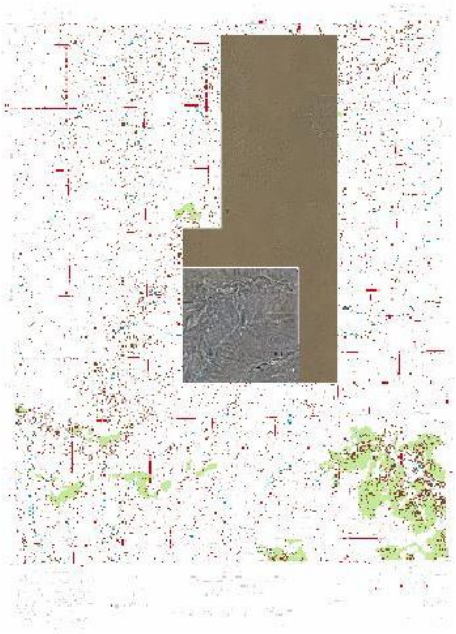

Figure 4 Pueblo Precision Bombing Range #2 wide-area survey site within Packer's Gap 1:24,000 USGS topographical map (7 ½ Minute Quadrangle Sheet**)**

Figure 5 Vegetation typical of the Pueblo PBR #2 area. [9]

Historical Usage and Suspected Targets. The training range consisted of a bombing camp with two runways and nine precision bombing targets, a suspected 75 mm air-to-ground target, along with an air-to-ground pattern gunnery range. A map displaying these locations is shown in Figure 6. This knowledge can be utilized to generate a feature map indicating high likelihood of UXO contamination at known target sites and some likelihood at suspected target sites.

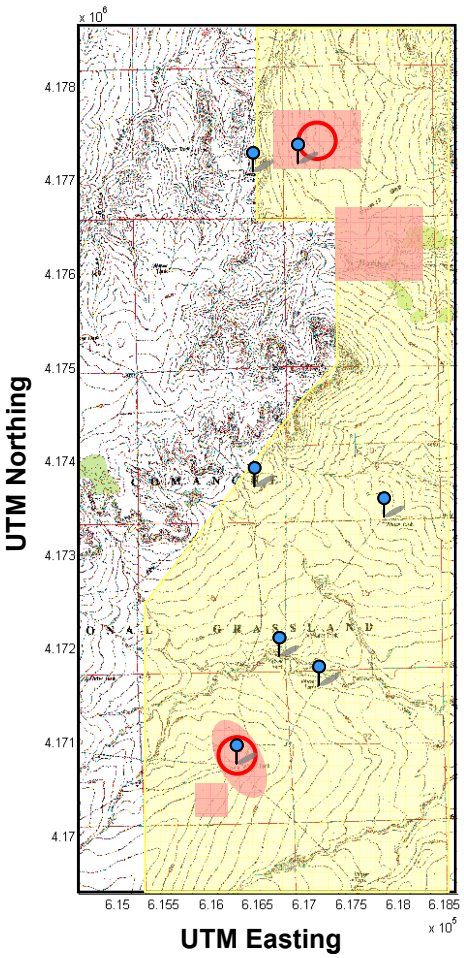

Figure 6 Pueblo PBR #2 topographical map showing the survey area (yellow), man-made structure locations (blue dots), and known and suspected bombing target and gunning range areas (red).

Geological Summary. The presence of sedimentary rocks and the lack of iron-bearing and magnetic minerals [11,12] in the study site mean that minimal effect, if any, will occur with the magnetometer data. The main geologic structures (domes, synclines) are far enough away from the area to also not affect the magnetometer data. Any effects on the data will come mainly from any man-made features in the area (e.g., trucks or other equipment left by surveyors, electric lines, fences, and pipelines).

Although the Pueblo site contains minimal magnetic geologic features, the following effects on magnetometer data have to be considered for future study sites: (1) magnetic ore bodies either exposed as an outcrop or beneath the surface; (2) large geologic structures containing magnetic minerals (magmatic intrusions); (3) soils that contain significant amounts of magnetic iron-bearing minerals; (4) volcanic rocks containing significant magnetic minerals that produce magnetic anomalies; (5) structures that occur at tectonic plate boundaries (magnetics can be positive or negative) (6) fault zones, and (7) anticlines and synclines that effect the location and concentration of rocks containing magnetized minerals.

Physiography, Relief and Drainage. Otero County lies within the physiographic province of the Great Plains. The relief is gently undulating. The elevation ranges from 3,965 feet in the northeast to 5,150 feet on a high mesa in the south-central part of the county for a total relief of almost 1,200 feet across the site. Otero County is drained by the Arkansas River and its tributaries. Major tributaries of the Arkansas river in Otero County are the Apishapa River, Timpas Creek, Crooked Arroyo, Anderson Arroyo and King Arroyo. [13] The vegetation is typical of the Great Plains. The rolling surface contains bunch grass, sage, scattered cactus and yucca. There are scattered low trees and bushes in several areas. [14] The information obtained indicates that the surface topography probed by LiDAR will be dominated in many portions of the site by washes, rolling hills, and bluffs. A lack of large vegetation (e.g., trees) within the survey site indicates that a relatively high value can be placed upon the acquired LiDAR data, as the extensive application of a ground cover cancellation algorithm was not required.

Ground Truth Data. In the summer of 2006, SERDP and ESTCP personnel conducted a ground-truth survey of the Pueblo site in order to provide data with which to validate Wide-Area Assessment Pilot Program results. These data were obtained by project MM1510 researchers and is depicted in Figure 7.

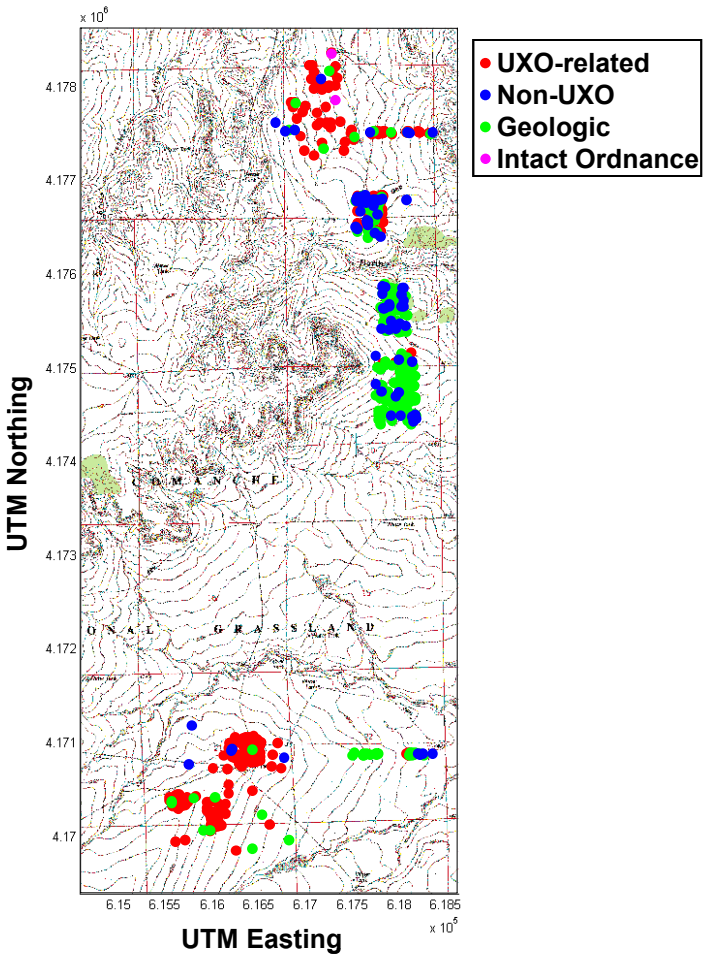

Figure 7 Pueblo PBR #2 topographical map with ground truth data. Red dots indicate locations of ordnance-related, blue dots indicate non-UXO scrap, green dots indicate geologic feature (i.e., an empty dig site), and magenta dots indicate locations of intact ordnance.

Evaluation of Current Sensor Algorithms

For orthophotographic data, a wide variety of ground cover classification algorithms have been reported in remote sensing literature.[15-19] These algorithms usually center on texture analysis and pattern recognition schemes for discerning ground cover type. Current literature reports of automated analyses of aerial imagery tend to focus on texture mapping, ground cover classification and detection of anomalies. No applications specific to wide-area assessment of UXO were reported. This result is not surprising as aerial photography is not capable of directly probing UXO objects, but must instead be used to locate visible features that have a high probability of co-occurrence with UXO. With this goal in mind, it is possible that ground cover classification could be useful in distinguishing foliage and geologic features from ordnance-related features.

LiDAR survey data were provided by Sky Research both as “raw” surface altitude measurements of the surveyed region and as data processed with ground cover

cancellation algorithms that estimate the surface altitude measurements as "bare earth." Both versions of the data were also provided as shaded relief visualizations. While the shaded relief versions were advantageous for visual inspection of the data, they were not used for subsequent image analysis and feature extraction as the shading unnecessarily complicated automatic numerical analyses. This difficulty with shading is due to the choice of lighting angle in the shaded relief map. The lighting angle is essentially an arbitrarily chosen parameter and results in a variety of different potential images from the same surface estimate. In contrast, the "bare earth" estimation algorithm employed by Sky Research was effective at enhancing UXO-related features as compared to background and was used in subsequent analyses.

A literature review was performed to assess state-of-the-art sensor data algorithms for detection of buried unexploded ordnance with aerial LiDAR sensing. The review revealed that such applications of LiDAR topographical analysis are relatively new and under-reported in the scientific literature. Applications detailing various ground surface estimation methods were predominant in the current literature, with the subsequent topographical analyses often performed in a more or less manual fashion. Topographical applications were generally divided between environmental monitoring [20-26] and topographic mapping of urban areas. [27-31] Environmental monitoring included tasks such as quantitative assessment of beach and wetland erosion, [20,21] assessment of forest and rangeland ground cover, [22-24] and accurate topographical mapping of remote areas, such as underwater coral reefs [25] or texture analysis of polar sea ice. [26] Urban mapping applications included tasks such as building, [27] bridge, [28] and power line recognition [29] and three-dimensional modeling of man-made structures. [30,31]

Typically, the analysis procedures and/or algorithms utilized in each application were highly specific to the goals of that application, and consequently not directly applicable to wide-area UXO assessment. In some cases, the use of specific families of mathematical transforms, such as wavelet decomposition [32-34] and fractal dimension analysis [35] have been reported as part of preliminary work to determine their effectiveness at feature extraction. In these cases, the features examined and thus, the utility of the approaches, were also specific to the given applications. What does become apparent in a review of current literature, however, is that the general approach to topographical analysis of LiDAR data follows the same general steps in each case, regardless of application: First, a set of objects of interest was defined for the task at hand. Next, the manner in which these objects uniquely present themselves as perturbations in the raw LiDAR data cloud, or in the LiDAR-generated surface was discerned. This knowledge was then used to create a feature extraction algorithm that located regions of the LiDAR survey that were associated with the objects of interest. Although there appeared to be no "turn key" approaches to extracting UXO-related features from LiDAR survey data, an approach that followed the steps above while minding the context of other applications should provide the best chance for success.

The literature on helicopter and ground magnetometry focused largely on individual object detection. Such techniques are not necessarily well-suited to the task of wide-area assessment. Typical electromagnetic induction and total field magnetometry data

analysis algorithms utilize physics-based modeling to predict target size, orientation, and depth. [36-40] A number of pattern recognition and statistical techniques, [37,38,41-43] data fusion approaches, [44,45] and factor analysis algorithms[46,47] have been investigated to discriminate between UXO and non-UXO signatures. Most applications of multivariate analysis involved time and/or frequency domain EMI data, rather than TFM such as that acquired in the ESTCP WAA Pilot Program. Several tools that have been developed to assist in the analysis of magnetometry data are incorporated into a module for *Oasis Montaj* from GeoSoft, Inc. [48]

The utilization of physics-based modeling tools is often problematic when confronted with a high density of metallic objects, metallic clutter and magnetic geological features. [49] Therefore, much of this current research focuses on the development of algorithms and filters to deconvolve multiple signals. While the output of these algorithms may prove useful, their goals are not entirely consistent with wide-area assessment where the determination of areas of likely contamination takes precedence over identifying individual items of UXO. For instance, the identification of ordnance size and orientation is less important than simply determining whether the signal is or is not the result of UXO-related scrap. Thus, the application of these algorithms holds value in so much as it may provide information that assists in discriminating UXO from non-UXO signatures. Unfortunately, due to the immense size of potential wide-area survey sites, the computational complexity of analysis algorithms becomes a concern and the problem must be approached from this mindset, rather than from that of a limited, local area assessment. For this reason, the approach taken in this work focused on a morphological analysis of the observed signal in TFM survey data.

Feature Selection to Optimize Information and Pattern Recognition Implementation

Orthophoto Data Analysis. An examination of the orthophotographic data available for the former Pueblo PBR #2 was performed to ascertain the potential for automated feature extraction of UXO-related phenomena.

The main features depicted by the orthophotographic survey of the site were different types of ground cover, evidenced by color and shape morphology. Subjects such as dirt roads, trees, and brush were plainly visible. An orthophoto image at one-meter resolution of a sub region of the survey site is depicted in Figure 8.

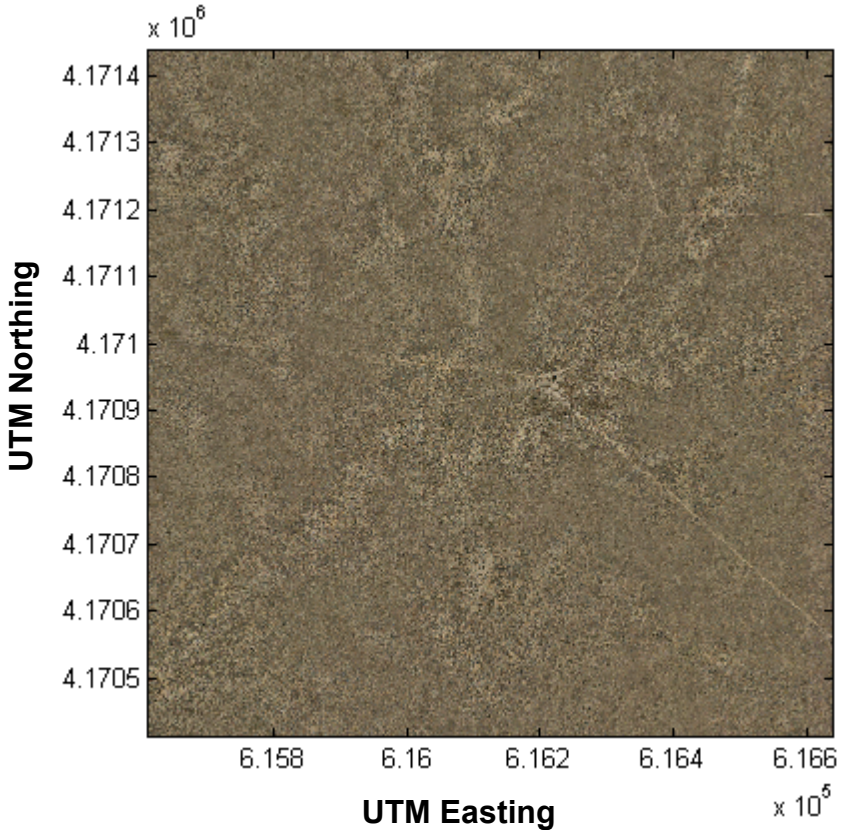

Figure 8 Orthophoto of a sub region of the Pueblo PBR #2.

Unfortunately, none of these features seemed to bear any useful association with UXO objects. In areas with heavy cratering, it was observed that vegetation was present within the craters, although vegetation was also observed in areas without cratering, negating this feature's usefulness for UXO indication. While the location of man-made structures such as fences and buildings was useful in assisting in the interpretation of magnetometry data, an automatic means of doing so was frustrated by the highly variable background present in the orthophotography images. Searching for regular geometric shapes (circular targets, fenced areas, buildings and structures) was difficult, as edges were generally very poorly defined. This was due in part to the relatively low contrast of the image as well as to the variability of the background. Additionally, an examination of the relationship

between color intensities on a pixel-by-pixel basis indicated a high degree of correlation, shown in Figure 9. This indicated that the orthophoto images contained very little information in terms of color.

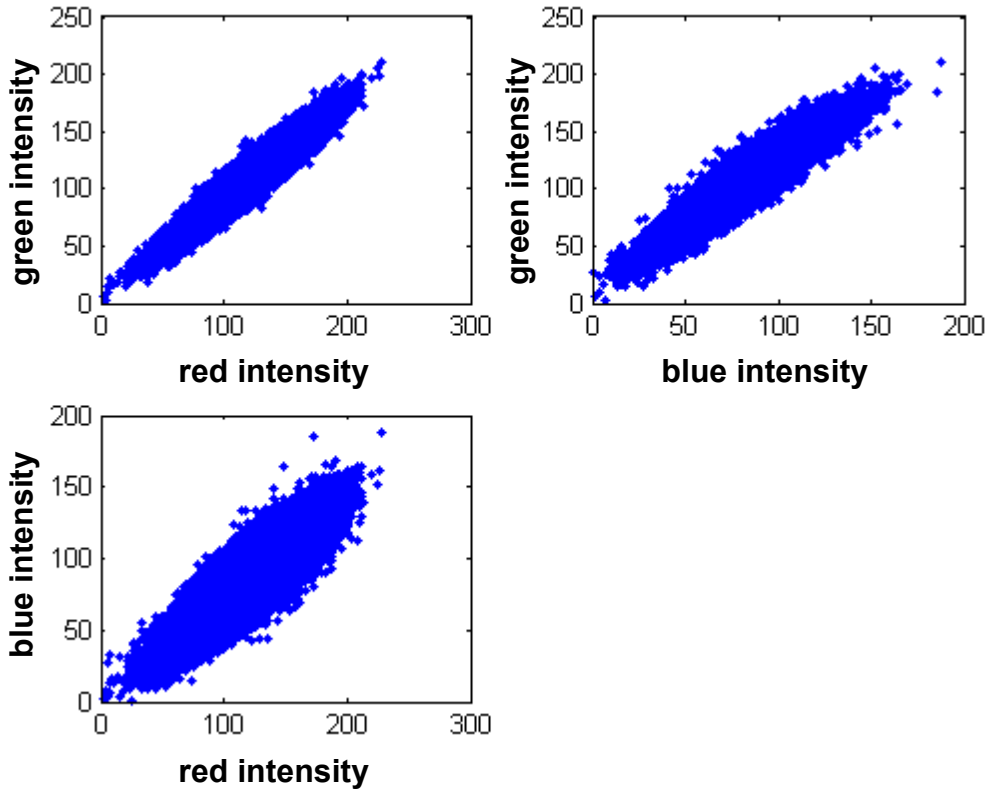

Figure 9 Depiction of the relationship between the three color channels of the orthophoto image shown in Figure 8 on a pixel-by-pixel basis.

A black and white version of the image in Figure 8 is shown in Figure 10. This image was generated by converting the 8-bit RGB image to an 8-bit grayscale image and then applying an intensity threshold of 130 units. The map depicts areas within the image that are lighter than their surroundings, but does not provide a path to locating features of interest for wide-area UXO assessment.

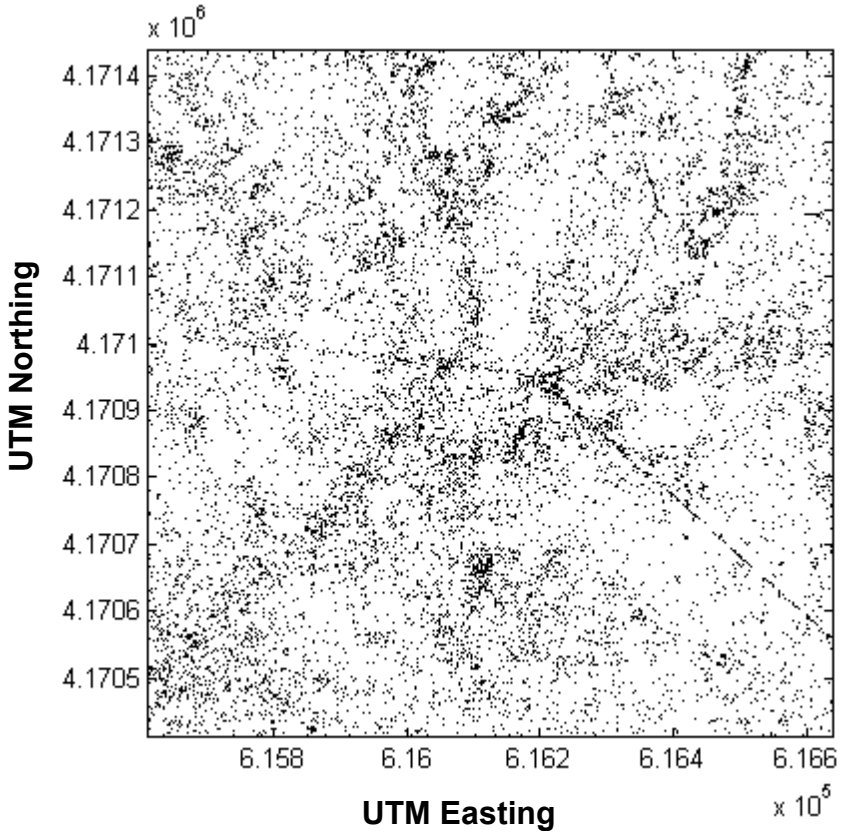

Figure 10 Black and white thresholded version the orthophoto image in Figure 8.

In an attempt to mitigate the effects of correlation between the three color channels of the orthophoto image, PCA [50] was used to transform the original RGB space into potentially more relevant descriptors. The first principal component of the image shown in Figure 8 is shown in Figure 11. As can be seen, the image is segmented into lighter regions (roads, bare earth) that are shaded blue in the false-color image in Figure 11, medium regions (grasses), shaded green and yellow, and darker regions (dense vegetation, water), shaded red. As was expected, subsequent principal components provided negligible information due to the high-degree of correlation between the color channels of the original image.

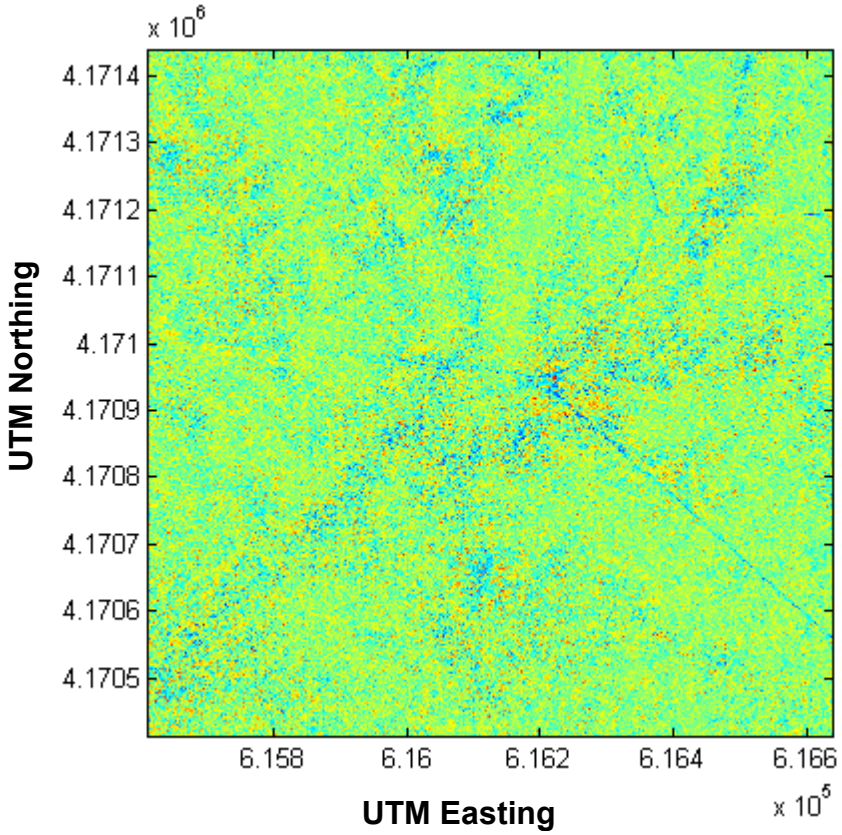

Figure 11 Image segmentation of the region depicted in Figure 8 via principal components analysis.

Unfortunately, information obtained from ground cover classification methods provided no clear path to improving UXO assessment in any automatic fashion. Thus, the potential utility of this data set in wide area UXO assessment of the Pueblo PBR #2 is currently limited to assisting in visual assessment of the survey area. For example, an overlay of site imagery would assist in compiling expert information into maps for inclusion into a data fusion framework. Potential applications remain in utilizing image analysis techniques to identify features through classification of vegetation and ground cover, but only if such features are found to be correlated with ordnance-related objects, or, alternatively, correlated with prominent features in other survey data in such a way as they assist in the interpretation of that data.

LiDAR Data Analysis. The principal feature in LiDAR data associated with UXO is cratering of the ground surface. While unexploded ordnance itself does not cause crater formation, craters indicate a land usage pattern of active ordnance bombardment, and through the assumption of collocation, a commensurate increase in the likelihood that UXO is present. The two main criteria for a successful automatic crater detection algorithm are that it be reasonably fast and highly selective for ordnance-related craters.

It is important to note that the depth of the ordnance-related craters observed is small relative to the overall changes in elevation experienced within the survey area, as shown

in the shaded relief map in Figure 12 and in the top-down view shown in Figure 13(a). This means that the detection of craters must occur through the location of crater-specific arrangements of pixel values within the LiDAR image rather than directly through pixel values themselves. A popular algorithm used in machine vision for locating objects of radial symmetry is the circular Hough transform. [60] The output of the transform is a map of the same dimensions of the input image, with each pixel in the map indicating the output of an "accumulator" that sums the input data (or an appropriate transformation thereof, such as the output of a Sobel gradient edge detecting algorithm) occupying a constrained circular geometry about the pixel. Map pixels with a high accumulator value indicate areas at the center of a circular feature, and an appropriate threshold is applied to label these features.

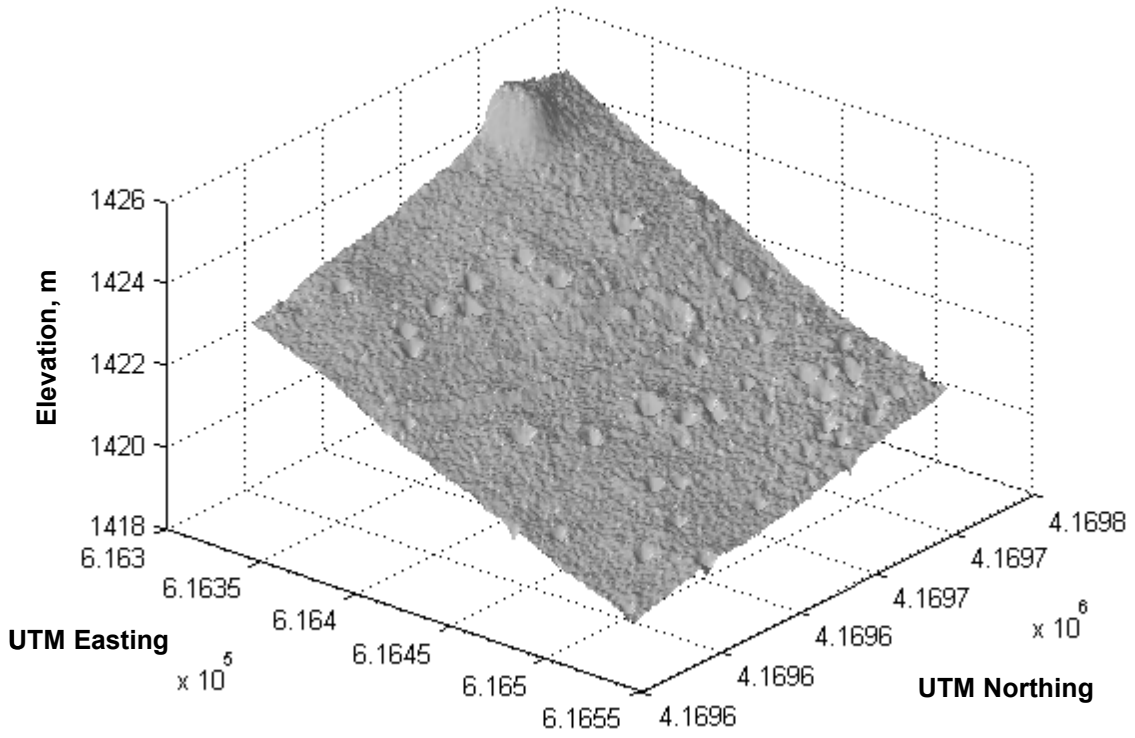

Figure 12 Subsection of LiDAR generated surface estimate for the Pueblo site showing ordnance-related cratering. Typical crater depths are smaller than variations in surface elevation.

Adapting this technique for crater detection, the initial LiDAR surface data needed to be transformed in order to give high signal value to crater slopes and low value to relatively flat areas. This was accomplished by estimating the gradient (i.e. the slope of the surface) at each pixel in the LiDAR image. Next, a moving window filter was applied across the gradient estimate image, accumulating signal at a fixed radius range from each pixel. This was implemented with functions from MATLAB's Image Processing Toolbox. An equivalent, but faster executing, implementation was available on MATLAB's Central File Exchange. [52] The alternate implementation used an estimate

of the gradient direction as well, adding to the accumulator of the pixel one radius unit away in the direction of the gradient. The approach is essentially the same as that used by Loy and Zelinsky.[53] In either case, the range of feature radii over which to search was specified. In initial testing, the two circular Hough transform implementations examined provided essentially equivalent output.

In order to assess the circular Hough transform's ability to detect craters within the LiDAR data, it was first applied to the subset of data depicted in Figure 12. Figure 13(a) shows a top-down view of the shaded relief map shown in Figure 12. This view is useful for visualization purposes, but not for automated feature extraction. Figure 13(b) depicts a false-color map of the raw LiDAR surface data of the same region. This map indicates that the dominant feature in this region is a hillside sloping downward from the northwest corner of the image to the southeast corner. The craters located within this region are difficult to see, as they represent a small change in elevation relative to the terrain present at this location. A surface gradient estimate was calculated for every pixel in this image, which is shown in Figure 13(c). Here, the crater walls are clearly visible against the relatively small slope of the surrounding area. Finally, Figure 13(d) depicts the output of a circular Hough transform applied to this data. Crater locations are clearly visible and are selectively detected against other surface features, such as small hills and roadways. Further, the output of the circular Hough transform indicated that ordnance-related craters in this region were relatively uniform and were typically four meters across.

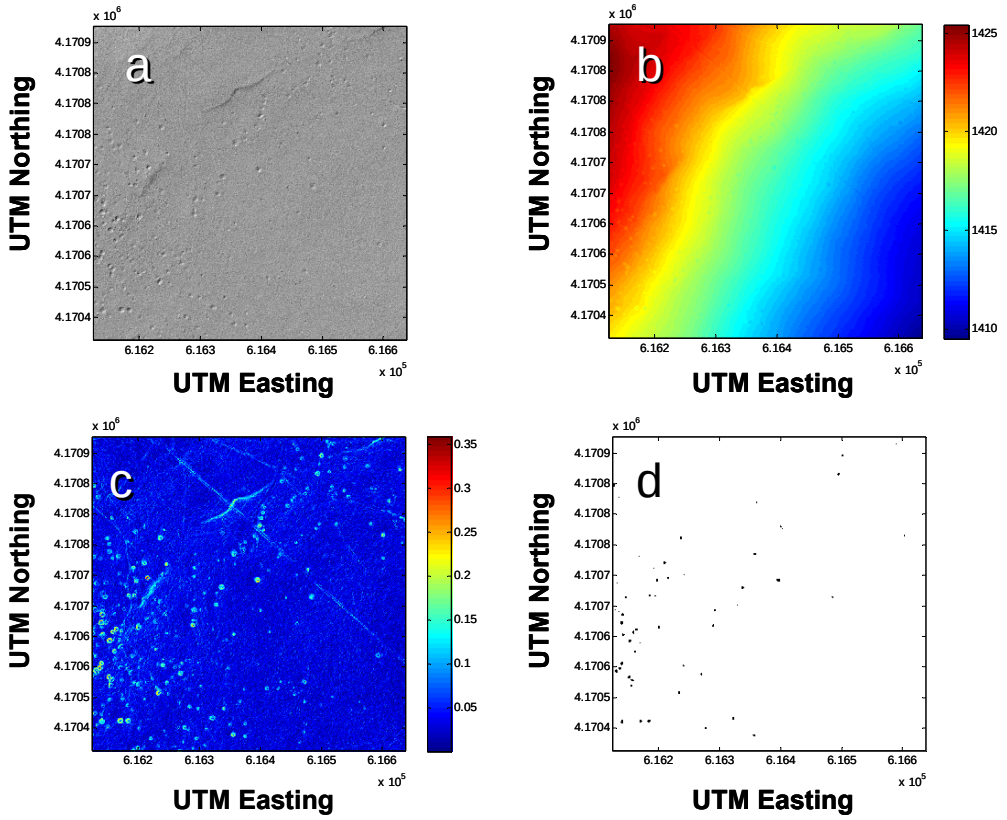

Figure 13 The process of applying a circular Hough transform to locate craters in LiDAR data. Figure 13(a) is a shaded relief map of a subsection of LiDAR data with ordnance-related cratering. Figure 13(b) depicts a false-color map of the raw LiDAR surface data, indicating that the dominant feature of this data is a hillside sloping downward from the northwest corner of the image to the southeast corner. In Figure 13(c) the MATLAB-generated surface gradient estimate is shown. Figure 13(d) depicts the output of a circular Hough transform applied to this data.

Following successful detection of craters in a heavily cratered region, the algorithm was next applied to the entire Pueblo site. The circular Hough transform output for the entire survey area is shown in Figure 14. As with the sub regions, craters are accurately located by the transform. Unfortunately, the crater detection algorithm also proved to be less selective than anticipated. As can be seen in Figure 14, large accumulator values were registered for various non-ordnance related geographic features such as gullies and bluffs, in the upper central portion of the region and elsewhere. This lack of selectivity was likely to hamper the utility of the circular Hough transform output for input into a data fusion based wide-area assessment framework.

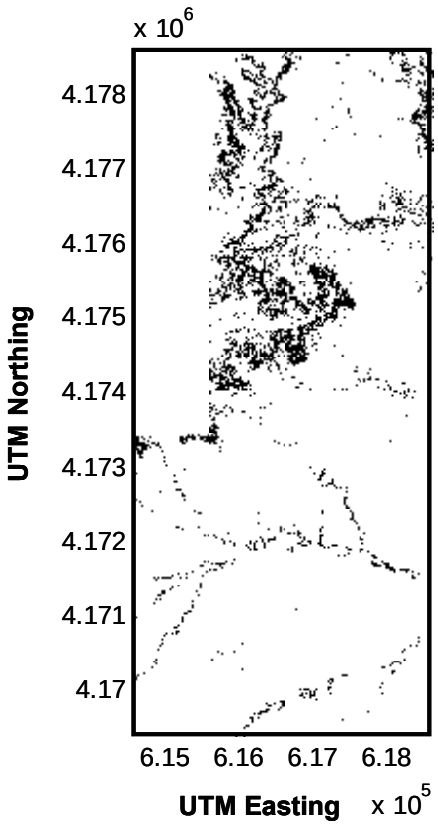

Figure 14 Survey-wide map of circular Hough transform output. The circular Hough transform demonstrates a significant response to non-ordnance related features in the upper region of the survey.

In response to this challenge, a more restrictive algorithm was implemented within MATLAB. First, the gradient and gradient direction for each pixel in the raw LiDAR surface were estimated, shown in Figure 15(a) and (b). This step was carried out in a similar manner to that utilized by Bai, Shen and Wang in their radial symmetry feature finding algorithm. [54] Pixels with gradient magnitudes less than 0.1 units were removed from consideration, resulting in the map shown in pane (c) of Figure 15. One consequence of this approach is that shallower, less steeply sloped craters will be more difficult to detect. The ability to detect shallower craters will depend on the surface texture of the survey site and the uncertainty in the LiDAR estimated surface. By specifying a particular crater radius range and surface gradient threshold, the crater detection algorithm can be utilized to selectively search for specific crater sizes. Expert information regarding soil density and depth as well as historical information regarding which types of ordnance were used at the site could conceivably be used to fine tune these parameters.

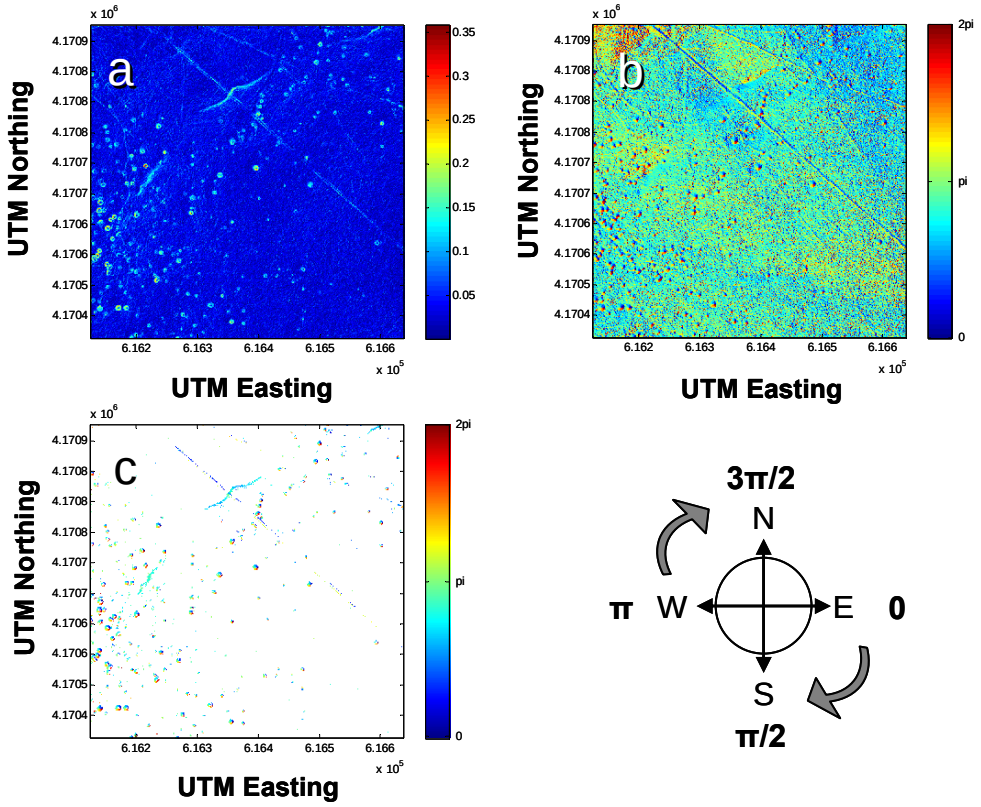

Figure 15 Estimated LiDAR surface gradient (a) and direction (b) before and after (c) gradient magnitude threshold application. (d) A direction of 0 radians indicates a positive surface gradient estimate orientation of due east.

Next, a windowed filter was applied across the gradient direction image that calculated the difference between the region local to the center pixel of the filter and an "ideal crater" gradient direction template. The crater template, shown in Figure 16, was generated by assuming a circular crater of radius four meters and calculating the direction of the surface gradient at each pixel in the hypothetical crater. Pixels that were in the center of the crater and beyond the rim were disregarded in this difference calculation. Pixels with gradients that were within 10 degrees of their counterpart in the crater template were located, with each one counting as one vote. The filter generated the number of votes each potential crater location garnered, normalized by the total number of potential votes. Figure 17 depicts the difference in direction between the crater template and (a), a non-crater region, and (b), a crater-containing region.

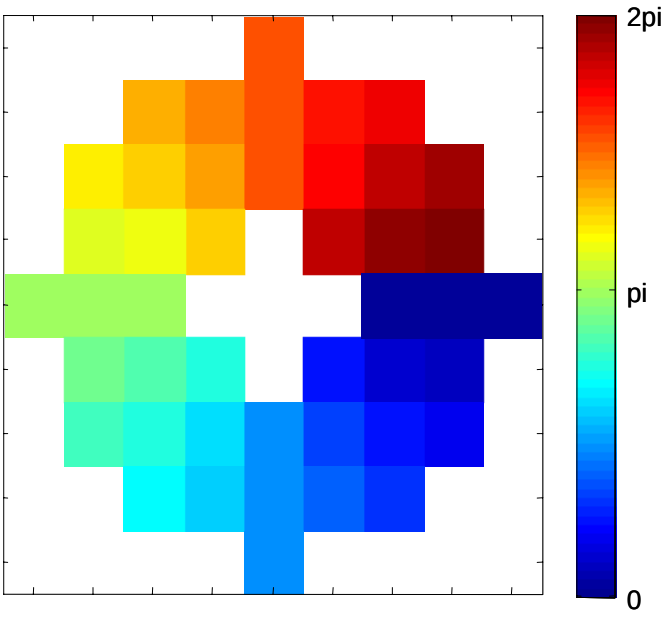

Figure 16 Surface gradient direction template for a crater of four meter radius in a one meter resolution image.

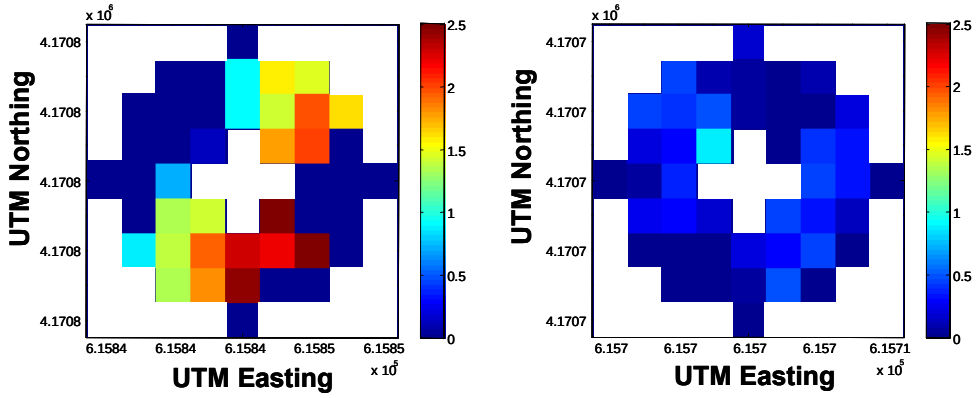

Figure 17 Residual between data and ideal crater template for (a) a non-crater containing region, and (b) a crater containing region.

Pixels with a value of less than 0.30 (only thirty percent of surrounding pixels point inward to center) were discarded and the remaining pixels were flagged as crater center locations. This method greatly enhanced rejection of geographic features within the survey area when compared to the circular Hough algorithms examined first, as demonstrated by the survey-wide algorithm output shown in Figure 18(a).

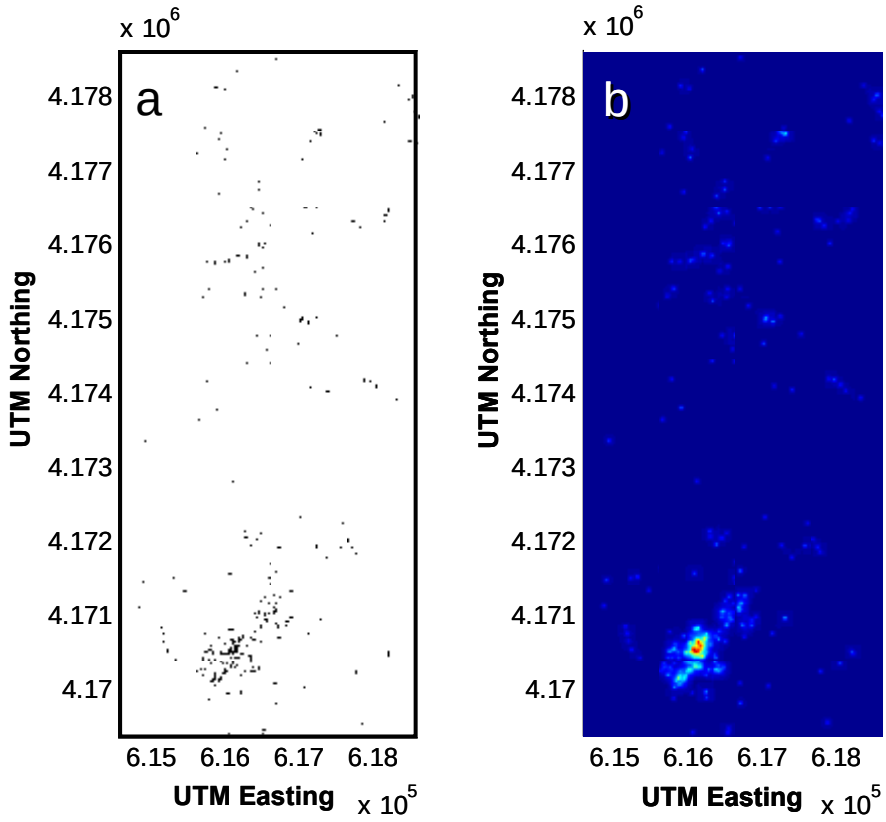

Figure 18 A survey-wide map of the crater-detection algorithm output is shown in (a) with crater centers dilated to enhance visibility. Shown in (b) is a map of estimated probability density for the crater distribution in (a).

The final step in the crater detection algorithm was to estimate the probability density of the crater feature found throughout the Pueblo survey area, shown in Figure 18(b). The information provided by the custom crater detection algorithm is now suitable for input into high-level data fusion algorithms. Additional data quality metrics such as crater depth and edge slope statistics can also be easily calculated for data fusion purposes. These metrics may become important in situations where distinguishing between different types of ordnance usage and/or ordnance and non-ordnance sources of cratering are desired.

Magnetometry Data Analysis. The phenomena measured via airborne magnetometry sensing are deviations in the background magnetic field of the earth due to the presence of ferromagnetic materials on or below the surface of the ground. Ferrous materials that may be present at a survey site include not only UXO and ordnance-related scrap but also a background of non-UXO related signal comprised of man-made features such as buildings, fences, pipelines, general metallic detritus, and magnetically active geological features. Thus, the main criterion for a successful detection algorithm for wide-area assessment of ordnance-related material is the accurate separation and extraction of UXO-related signal from background with computationally-reasonable methods.

Typically, analysis of magnetometer readings involves fitting a physics-based model to predict quantities such as object depth, size, and orientation. This approach can be complicated by highly overlapped signals from multiple objects and from excessive distance between the object and the sensor. For the purposes of wide-area assessment, it was decided that, rather than approaching the UXO recognition from a physics-based modeling approach, it would be advantageous to consider the problem from an image analysis standpoint, examining the morphological characteristics of total magnetic signal distributions throughout a given survey site. This approach has the potential to loosen requirements on magnetometer data gathering and to speed analysis times while continuing to provide useful assessments of potential UXO contamination for input to a data fusion framework.

During registration to the site map grid, the magnetometer signal readings were converted to absolute value to provide a total magnetometer signal at each pixel. These magnetic data are shown in Figure 19 for the Pueblo site. This total magnetic signal was then examined to look for features that would separate ordnance-related signal from the ferromagnetic background.

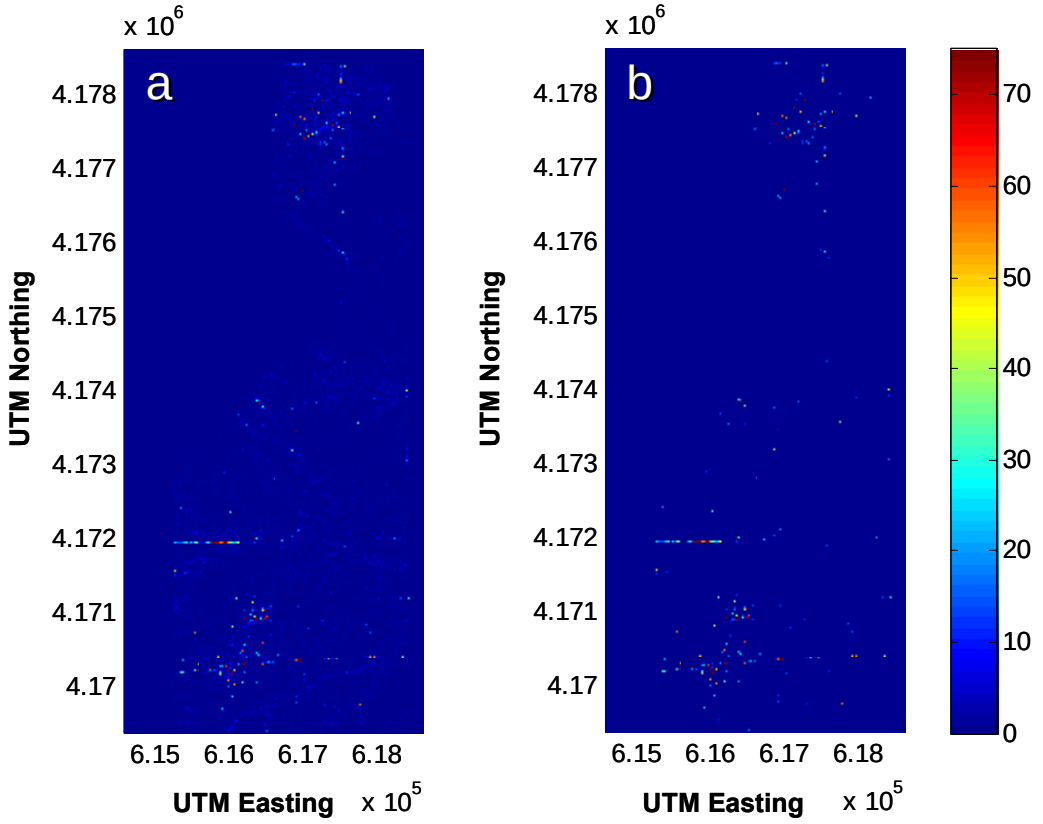

Figure 19 Estimated total coverage magnetometry survey constructed from airborne magnetometry data acquired over the Pueblo site. Depicted are (a) absolute magnetometer reading, and (b) absolute magnetometer reading with a threshold of 10 nT applied to exclude signal due to magnetic geology.

The principle algorithmic challenge to feature detection within the magnetometry data is the similarity of the ordnance-related signal to the non-ordnance background, both in terms of feature intensity and spatial location. Figure 20 displays magnetometry data from the southern portion of the Pueblo site, illustrating the similarities between ordnance-related signal associated with a ship target berm (outlined in red) and non-UXO related ferromagnetic objects such as fence lines and other surface structures. Figure 21 shows a zoomed view of these items. Figure 22 displays the magnetometry data related to these features at even finer detail, exposing their similarities. As can be seen in these figures, a scatter cloud of semi-circular clusters of pixels corresponding to ordnance-related signal is located near the ship target berm. The morphology of the cloud exhibits circular symmetry over several size scales, but is incongruous with the linear morphology of the fence with which the cloud overlaps. Therefore, an initial examination of the magnetic data was performed with a wavelet-based approach [55,56], which is typically well-suited to distinguishing shape and scale dependent features.

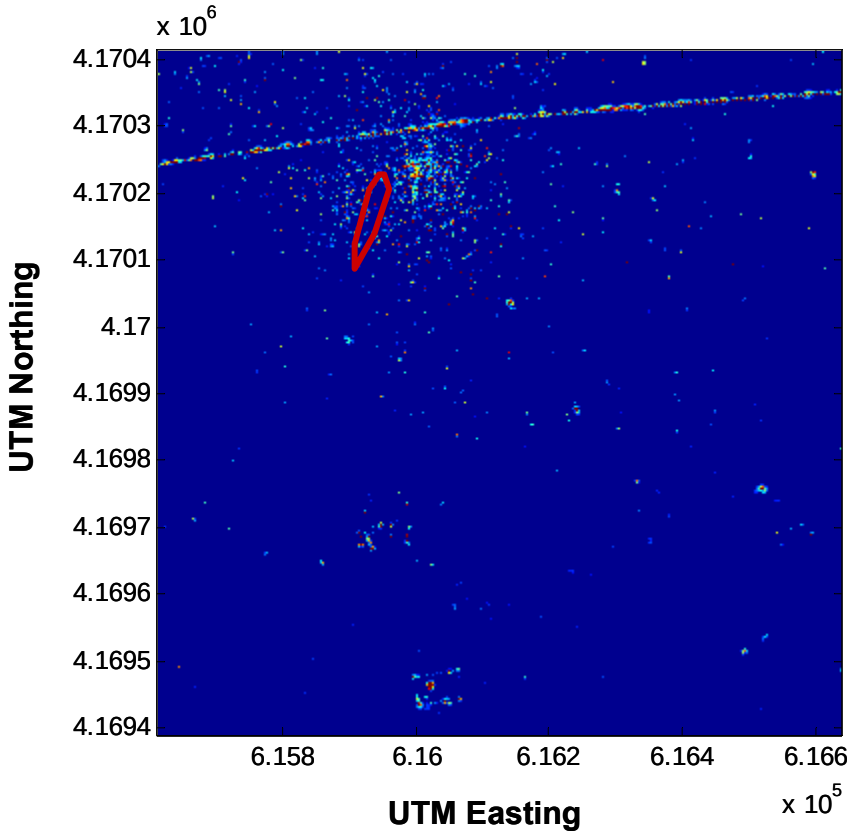

Figure 20 Subsection of the airborne magnetometry survey containing a ship target (indicated in red), ordnance-related scrap, and man-made structures.

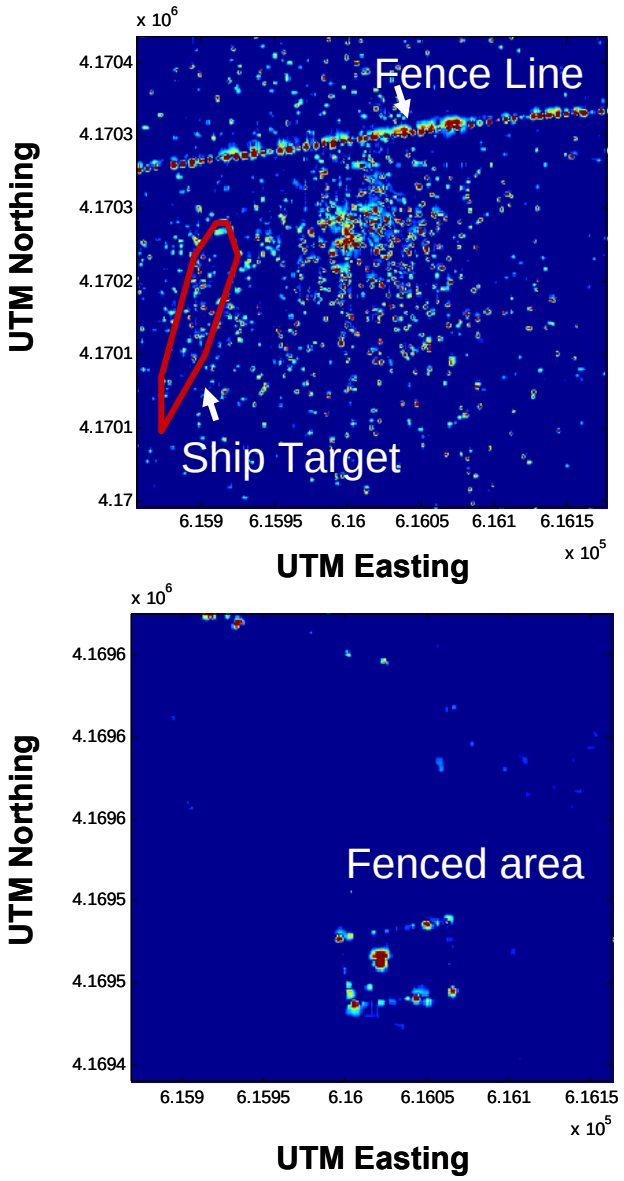

Figure 21 Enlarged regions of Figure 20 containing a ship target (indicated in red), ordnance-related scrap, and a man-made structures.

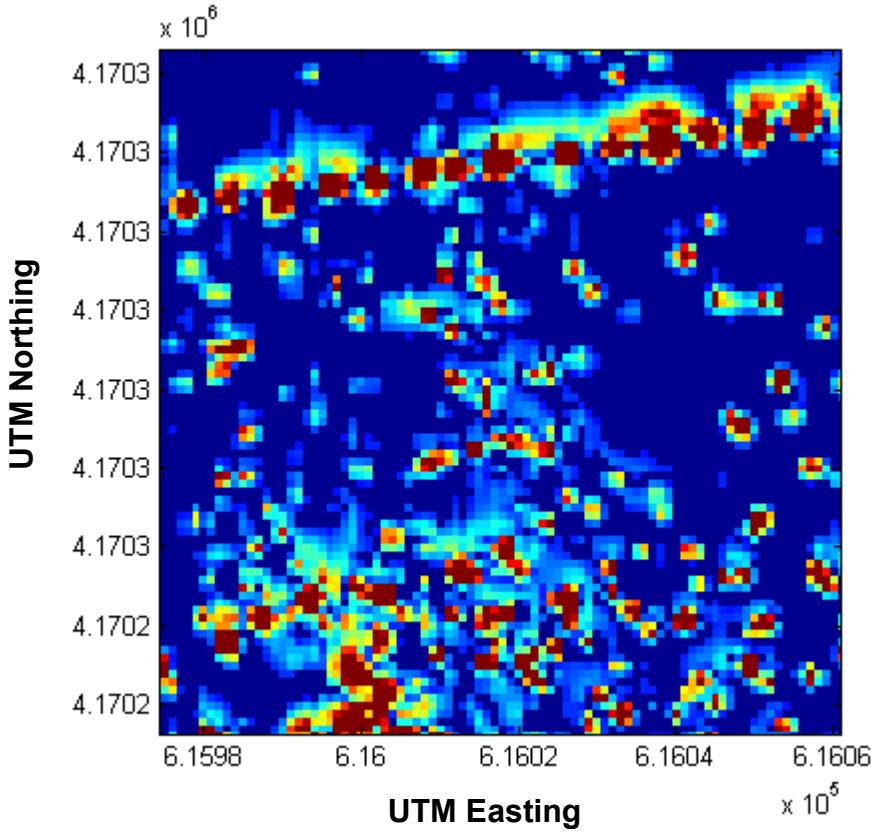

Figure 22 Further enlarged region of Figure 20 showing the data similarity of the scatter cloud and fence features.

Wavelet Analysis. The first step was to explore "denoising" of the wavelet decomposition of the magnetometry data. Denoising is an umbrella term in the signal processing community that refers to methods which remove portions of the signal, typically unwanted noise, but which can also be structured background features. Noise is generally captured by small-valued wavelets in finely detailed scales. Its removal was expected to enhance the semi-circular clusters of ordnance-related signal in the data. Large scale morphological features such as the scatter cloud and the fence line are generally captured by large valued wavelets at all size scales and were expected to be enhanced after the removal of the least significantly valued wavelets. The impact of removing small valued wavelets from the finely and coarsely detailed scales in the wavelet decomposition of the magnetometry data was examined after applying a standard wavelet denoising algorithm. [57,58] Even though several wavelet families and widely varying noise thresholds were applied, denoising of the magnetometry data did not enhance ordnance-related signal beyond that achievable by simply thresholding the magnetometry data at an intensity of ten units (i.e., keeping data with values greater than or equal to 10 nT). The threshold-applied magnetometry data are shown in Figure 19(b). Close comparison with Figure 19(a) shows that thresholding was effective in eliminating small valued and unstructured ferromagnetic background distributed fairly uniformly in the magnetometry data across the Pueblo site.

Though denoising was not effective at enhancing magnetometry features, it did reveal that the magnetometry data were of good quality in the sense that was relatively noise-free. Pixel intensities greater in magnitude than approximately one unit appeared to consistently correspond to ferromagnetic objects on or below the surface of the ground, rather than to sources of false positives specific to the magnetometry sensor system. By association, features in the magnetometry data should also be of similar good quality.

The next step in analyzing the wavelet decomposition of the magnetometry data was to look for morphological parameters that might characterize and distinguish the ordnance-related signal from the ferromagnetic background. Because the wavelet decomposition is multi-scale in nature, it is able to separate features by size. Therefore, the decomposition of the magnetometry data was examined to look for morphological features at size scales that might correspond to ordnance-related signal or ferromagnetic background, for example, a characteristic diameter for the semi-circular pixel clusters

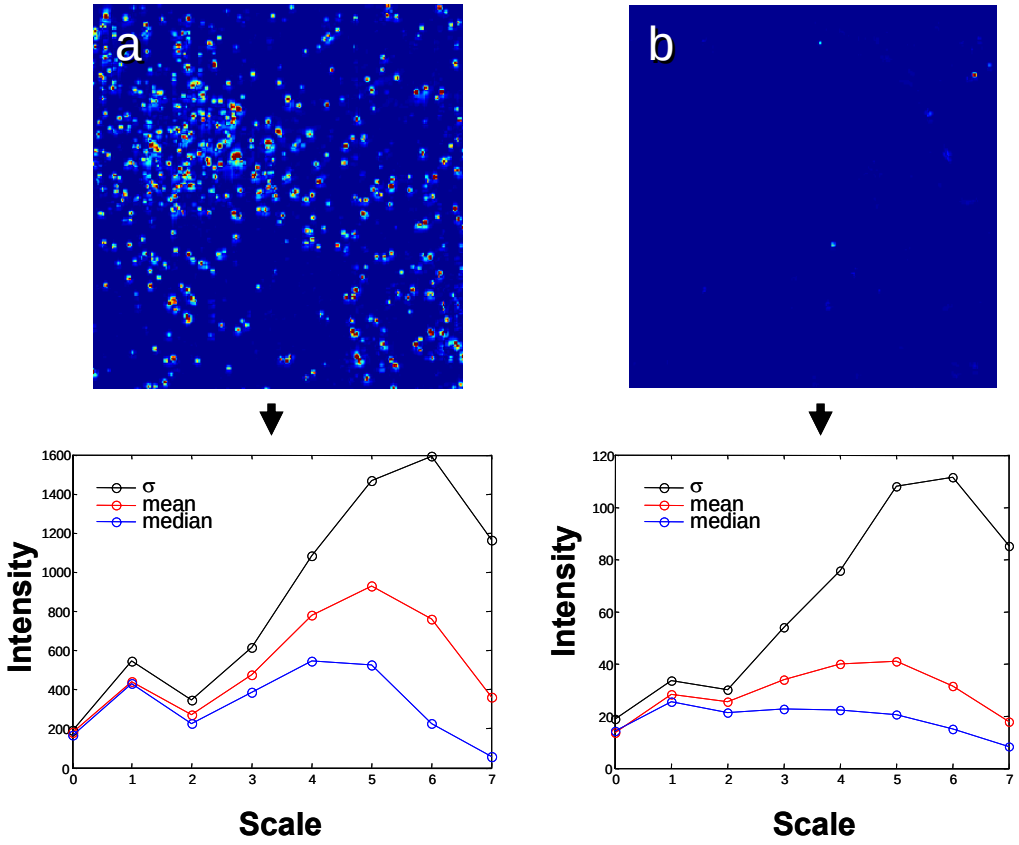

Figure 23 Example survey regions (a) with ordnance-related signal and (b) free of ordnance-related signal. For each region the corresponding standard deviation, mean, median values of wavelet coefficients per scale (0 = coarsest) are depicted.

Figure 23 shows a comparison of two small sections of the magnetometry data. The upper left pane (Figure 23(a)) shows a region replete with ordnance-related signal; the upper right pane (Figure 23(b)) shows a region nearly free of signal and ferromagnetic

background. The lower portion of Figures 23(a) and (b) shows plots the mean, median, and standard deviations of the wavelet decomposition per scale for the magnetometry data (a) and (b), respectively. Although each wavelet statistic curve exhibits a peak for the ordnance-related data, the peaks are rather broad and are not consistent with a single scale. Further, the overall profiles of the wavelet curves for the ordnance-related data are very similar to those of the background image, differing significantly only in magnitude. Thus, the wavelet decomposition analysis concluded that the semi-circular clusters of pixels representing ordnance-related signal in the magnetometry data typically comprised several size scales simultaneously and were so sparsely distributed that a better separator of signal from background was simply the pixel magnitude. This is also consistent with the earlier denoising results, that is, the lack of enhancement to magnetometry features.

Pixel Clustering Analysis. The next step in the analysis of magnetometry data focused on extracting features relevant for ordnance-related signal in the context of density, intensity, and morphology aspects to the data. Based on the results from the wavelet decomposition analysis, the magnetometry data were thresholded to ten units for this effort to remove spurious and small-valued background. An algorithm was developed to identify clusters of adjacent and above-threshold pixels and group them into "pixel islands." Adjacency was defined as the pixels eight nearest neighbors. An island was defined as any cluster of two or more adjacent and above-threshold pixels. Pixels meeting these criteria are shown in Figure 24(a) for the Pueblo site. Figure 24(b) displays a preliminary probability density obtained from the density of pixel islands in pane (a). A zoomed view displaying the pixel island components to the ordnance-related cloud and fence features from Figure 22 are shown in Figure 25(a). The binary version used to generate a probability density distribution is shown in Figure 25(b). Pixel islands are able to capture ordnance-related features in the magnetometry data, but significant ferromagnetic background from man-made structures is equally well-captured.

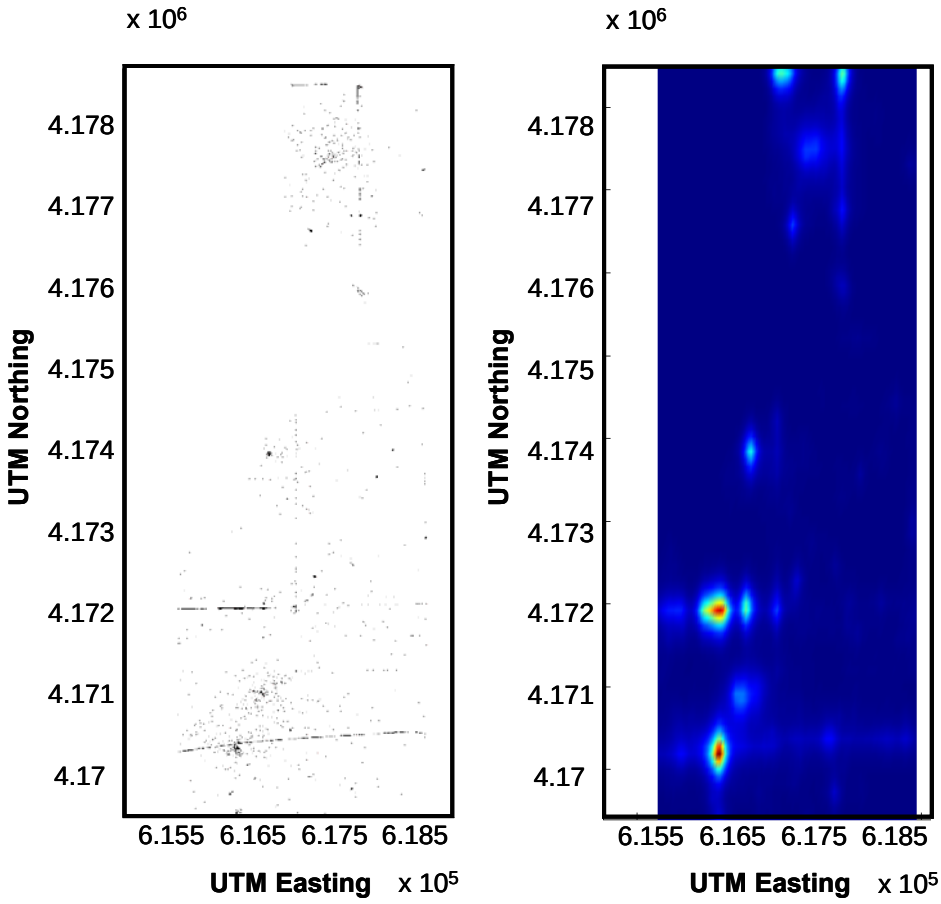

Figure 24 Shown in (a) are pixel islands in the magnetometry data. Figure 24(b) is a map of estimated probability density generated from (a).

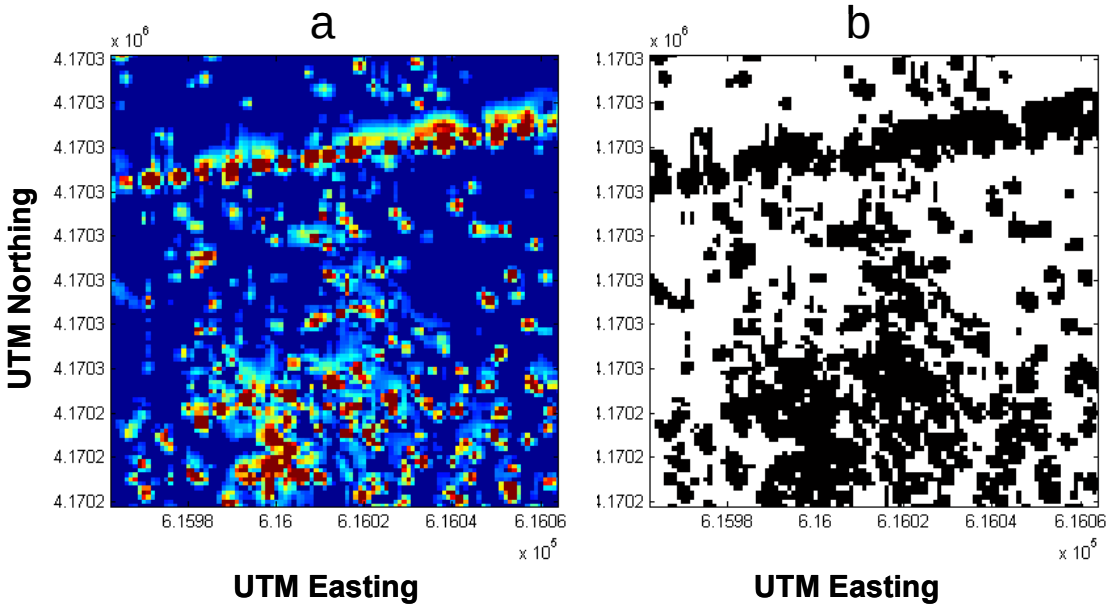

Figure 25 Shown in (a) are pixel island components to features shown in Figure 22. Figure 25(b) depicts a binary version of (a).

In order to distinguish ordnance-related features from structured ferromagnetic background, the morphology of the pixel islands was explored. Filtering pixel islands based on the number of pixels each island contained was effective in separating signal from background features. For example, Figure 26(a) displays all pixel islands in the southern portion of the Pueblo site shown previously in Figure 20. Figure 26(b) displays only those pixel islands with two to 75 member pixels. Note that only a few islands from the man-made structures remain. Panes (c) and (d) display pixel islands with 75 – 200 and 200 – 1000 member pixels, respectively. In these ranges, nearly all pixel islands belong to man-made structures. Only a few islands in the densest regions of the ordnance-related scatter cloud are present in these ranges. Figure 27(a) displays pixel islands with less than 100 member pixels for the Pueblo site. Figure 27(b) shows the corresponding preliminary probability density for this pixel island feature range. The scatter clouds of ordnance-related signal associated with targets in the northern and southern sections are clearly the dominant features. For comparison, results for pixel islands with more than 100 member pixels are displayed Figure 28. Although the densest regions of the scatter clouds are visible, the features in Figure 28 are almost entirely due to man-made structures, with the fence line crossing the southern section clearly visible.

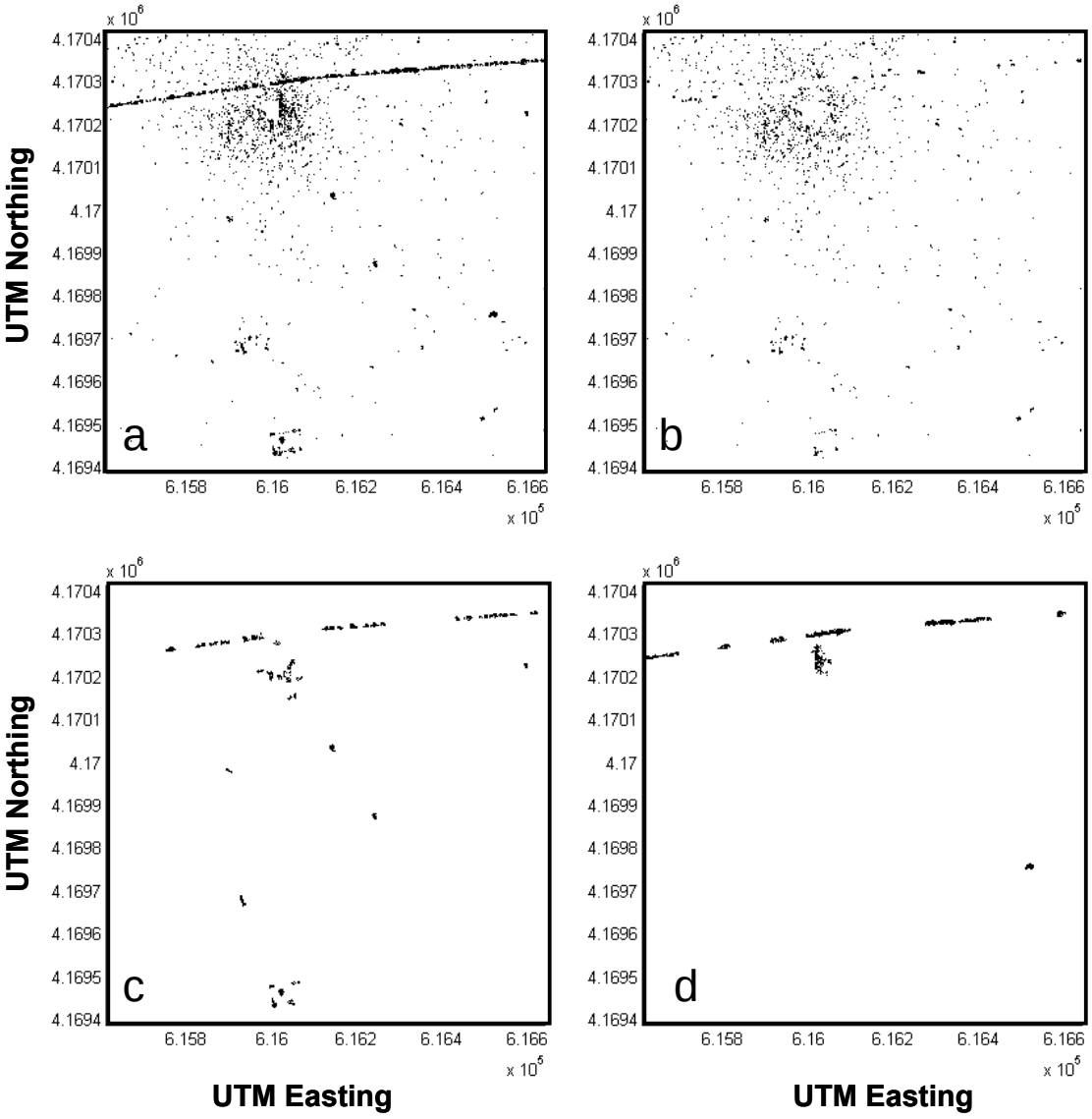

Figure 26 Filtering of pixel islands: (a) all pixel islands, (b) islands with 2 – 75, (c) 75 – 200, and (d) 200 – 1000 member pixels.

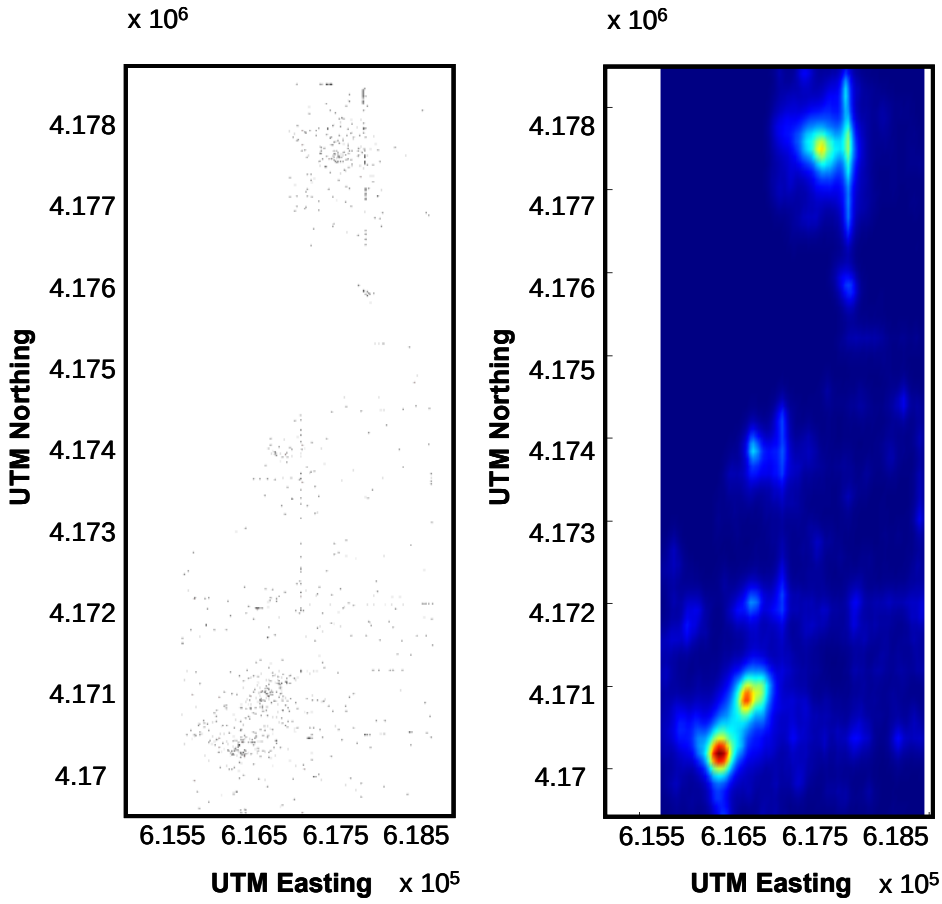

Figure 27 Shown in (a) are pixel islands containing less than 100 member pixels. Shown in (b) is a map of estimated probability density generated from (a).

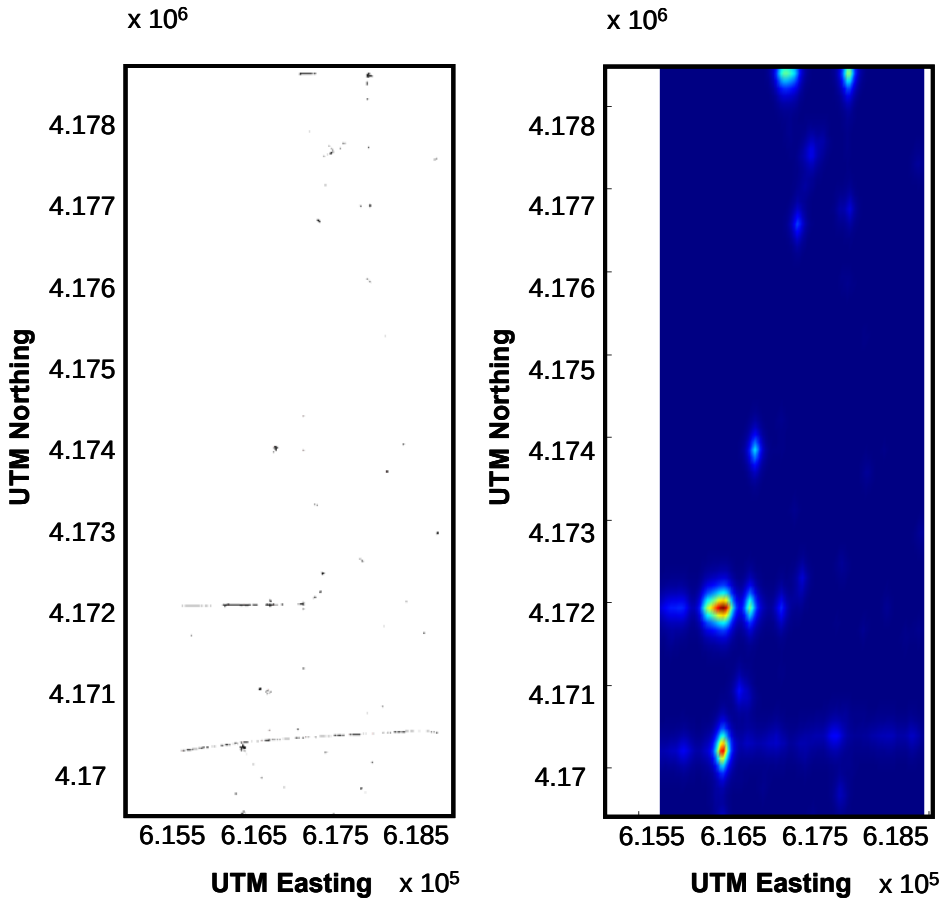

Figure 28 Shown in (a) are pixel islands containing more than 100 member pixels. Shown in (b) is a map of estimated probability density generated from (a).

The pixel island features contain additional information about the magnetometry data making possible further separation of ordnance-related signal from structured ferromagnetic background. First, the intensities of member pixels seemed to be larger for man-made structures than for ordnance. This could have been due to the location of structures on the ground surface, appreciably closer to helicopter than buried ordnance, as well as to more concentrated ferromagnetic content, typical of fence posts and pipelines. Figure 29 shows average pixel intensities for each pixel island in a sub region near the target in the southern region of the Pueblo site. Intensities in the fence feature were much higher than those in the dense cloud of UXO-related scrap around the bombing target. This approach may provide a probabilistic estimate to determine if features in the magnetometry data are on or below the surface of the ground.

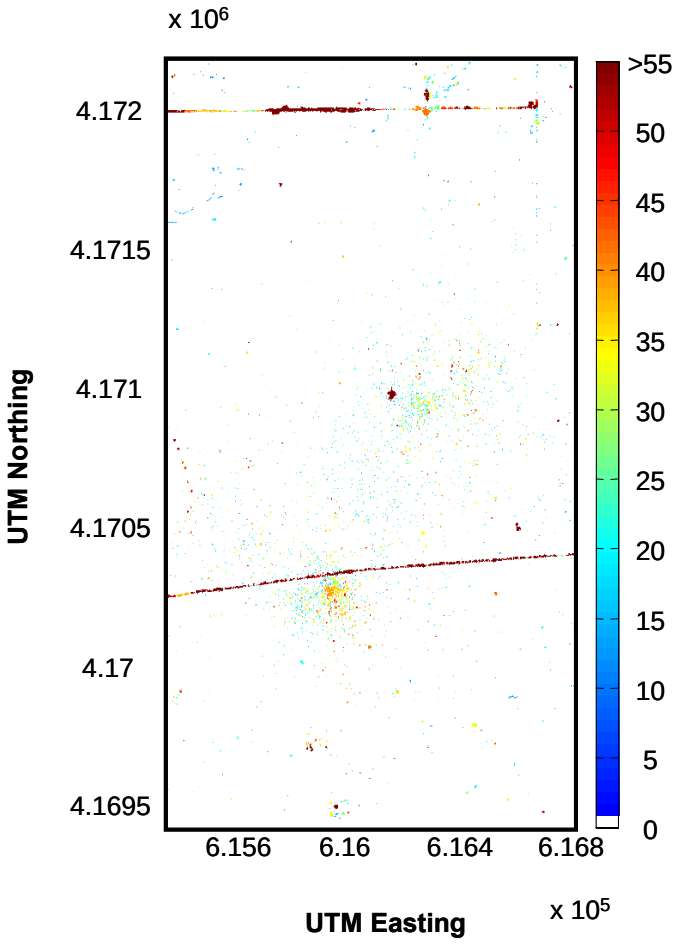

Figure 29 Average pixel island intensities, capped at 55 nT, for island pixels surrounding the target in the southern portion of the Pueblo site. Surface clutter objects such as fence lines have significantly greater intensity per pixel.

Figures 30 and 31 depict the distribution of pixel islands in the airborne magnetometer data with average signal intensities below and above a threshold of 50 nT, respectively. As with filtering based on pixel island size, good discrimination was observed between signal associated with buried UXO-related scrap and that associated with metallic objects on the surface.

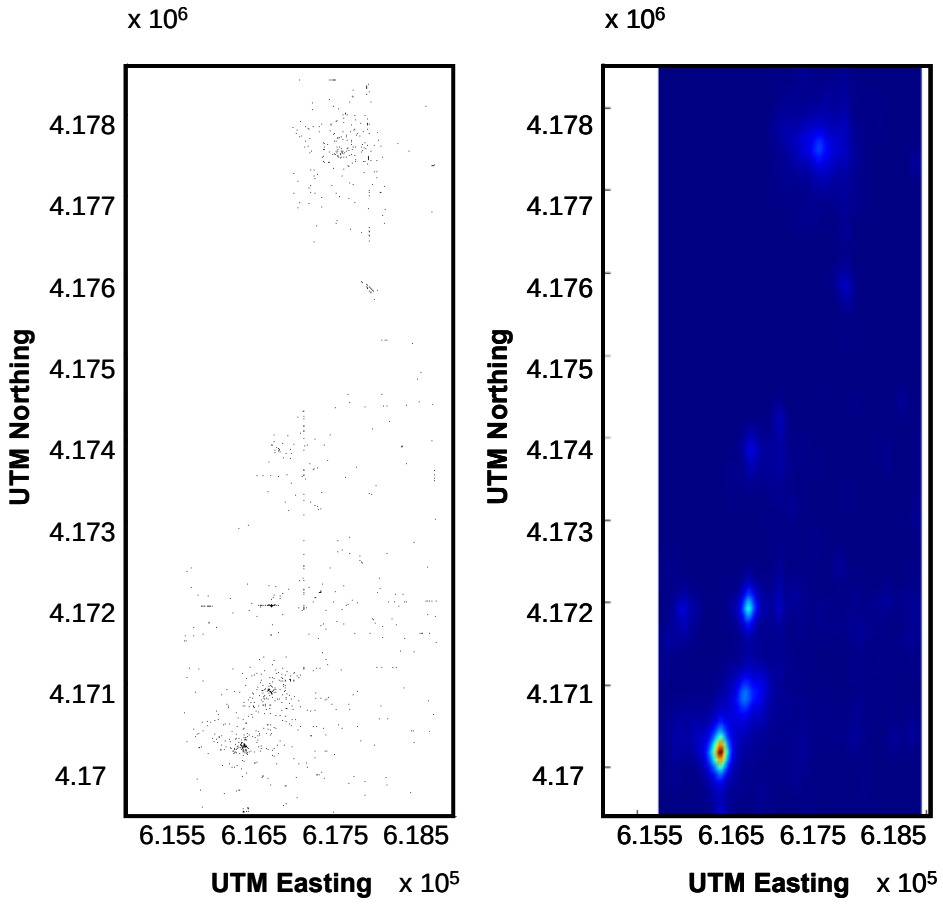

Figure 30 Shown in (a) are magnetometer signal pixel islands with average intensity less than 50 nT. Shown in (b) is a map of estimated probability density generated from the pixel islands in (a).

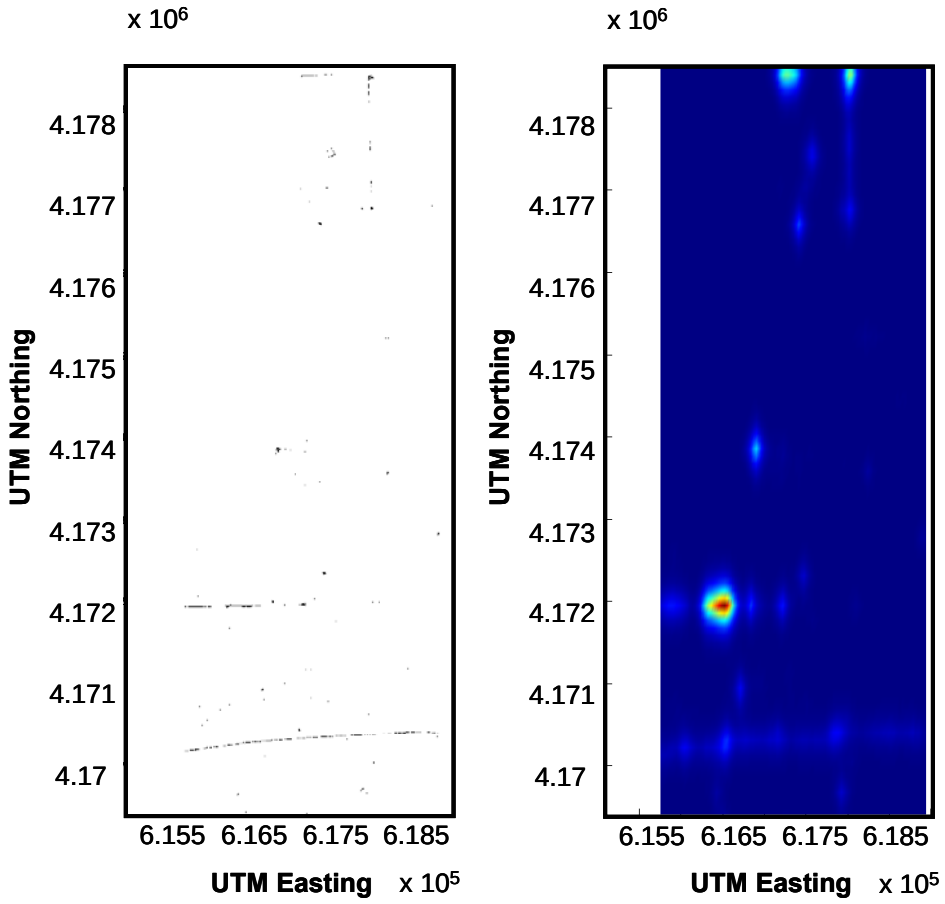

Figure 31 Shown in (a) are magnetometer signal pixel islands with average intensity more than 50 nT. Shown in (b) is a map of estimated probability density generated from the pixel islands in (a).

Second, the shapes of pixel islands associated with man-made structures such as fence lines were generally more elliptical than those in the ordnance-related scatter cloud. Figure 32, reproduced here from Figure 25(b), shows a binary image of the pixel islands shown in Figure 22. Islands associated with the fence tend to have a major axis that is much larger than their minor axis. It may be possible to build a filter based on this characteristic to help separate ordnance-related signal from ferromagnetic background. Taken as a whole, the magnetometry analysis resulted in three layers of extracted features that are expected to prove useful as inputs to the data fusion algorithms to be developed in year two of the project.

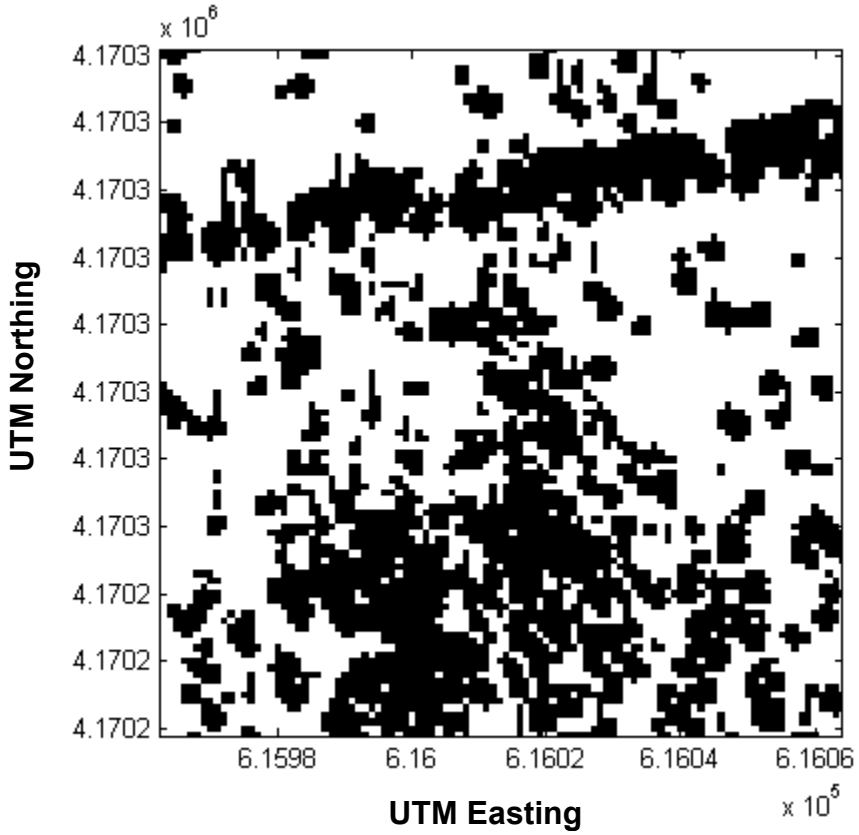

Figure 32 Binary version of Figure 22.

Summary of Results from Year One Tasks

NRL reviewed all the available data obtained from the ESTCP WAA Pilot Program survey of Pueblo PBR #2. This included magnetometry data acquired via helicopter survey, LiDAR data in two resolution scales from airborne surveys, and orthophotography data from airborne surveys. Efforts at importing and registering data of various formats into the MATLAB environment were successful. Utilities for the importation of arbitrary geo-referenced image data and text data in XYZ format were also constructed and tested. In addition, a displacement of approximately four meters in geo-reference information was discovered in the orthophotography data acquired in 2004 relative to other survey data. SERDP and Skysearch were notified and this discrepancy was addressed and successfully rectified.

NRL obtained and reviewed auxiliary information for the Pueblo PBR #2. This expert information was comprised of topological maps, geological survey data, and the archive search report. Historical usage indicated a training range with a bombing camp and nine precision bombing targets. Anecdotal information in the archive search report also indicated the presence of a suspected 75 mm air-to-ground target and pattern gunnery range. These data were utilized to generate a historical target feature map of likely UXO contamination. Geological survey data indicated that the Pueblo site contained minimal

magnetic geological features. Foliage and other ground surface features that may interfere with data acquisition were also minimal at the site. Such features are expected to significantly affect data acquisition and quality at other sites, and therefore will be incorporated into feature maps where relevant.

NRL evaluated the current state-of-the-art in data analysis and data fusion algorithms for the sensing technologies employed in the ESTCP WAA Pilot Program surveys. A literature review indicated that the current state-of-the-art was generally focused on algorithm development for the detection of specific objects, and was therefore more suitable for local area applications than for wide-area assessment. Algorithms for orthophotography data emphasized classification of ground cover type through texture analyses or pattern recognition. Though the Pueblo site lacked significant ground cover, these algorithms may be applied to orthographic data from other surveyed sites. For LiDAR, algorithms were specific to the applications, which were mostly environmental. However, the general approach used for algorithm development proved useful in feature analysis. For magnetometry data, algorithms focused on physical modeling as a method of the detection of individual objects and required sensitivities not attainable in helimag surveys. Approaches to data fusion typically applied multivariate analysis to time and/or frequency domain EMI data to distinguish individual objects as well. EMI is a data source not yet available for wide-area assessment.

NRL performed feature selection specific to each data source to optimize the extraction of information relevant for wide-area assessment. As part of this effort, NRL also developed and implemented pattern recognition algorithms for all selected features in the sensor data obtained from the ESTCP WAA Pilot Program surveys. Methods for feature maps suitable for auxiliary information were discussed above. Craters were the principal UXO-related feature of the LiDAR and orthophotography data, and total magnetic content for the magnetometry data. For the LiDAR and orthophotography data, the main components of the backgrounds to feature selection were geology, foliage, and man-made structures. For the magnetometry data, geology and man-made structures contributed to the background while foliage was not a significant factor.

Of the three survey data sets, the orthographic data were the least informative source for the Pueblo PBR #2. Extraction of craters was not nearly as efficient as with the LiDAR data, and the minimal presence of foliage and man-made structures at this site made positive identification challenging. Thus, autonomic pattern recognition yielded features with very low signal-to-noise ratios. Crater extraction from the LiDAR data was successful. An algorithm based on the circular Hough transform was able to extract a value of four meters as the characteristic diameter of craters at the Pueblo site. Further, a pattern recognition algorithm based on the morphology of the craters was developed to locate them in the LiDAR data. This information was then converted into a feature map describing the density aspect of craters. Feature maps describing the intensity and quality aspects to craters may also provide data fusion algorithms with additional discriminatory information.

Feature selection was most successful with the magnetometry data. The total magnetic signal approach quickly yielded a feature map that displayed all relevant ferromagnetic signals from ordnance-related material and man-made structures present in the data from the surveyed area of the Pueblo PBR #2. Due to the minimal geomagnetic features at the Pueblo site, a simple threshold proved effective in eliminating geologic background, which is expected to be more significant at other ESTCP WAA Pilot Program sites. A pattern recognition algorithm was developed to separate ordnance-related signal from the ferromagnetic background of man-made structures. This information was then converted to a feature map describing the density aspect of ordnance-related material. Separate feature maps describing the intensity and morphology aspects of the ordnance-related and man-made components of data are also expected to provide additional discriminatory information for data fusion.

NRL developed a multi-resolution algorithm for converting feature maps to probability densities, which are required for the proposed Bayesian-based approach to data fusion. The multi-resolution algorithm used a computationally-intensive approach similar to that of Parzen windows. A less computationally intensive, but correspondingly less accurate, alternative based on two-dimensional histograms of the data was used to generate the figures of probability densities shown above. The generation of probability densities is a key enabling component for data fusion work slated for year two.

NRL also explored methods and algorithms for locating feature correlations among the various data sources. Visual inspection of data from the three surveyed sources revealed apparent spatial collocation of crater and ferromagnetic features. To quantify these correlations, principal components analysis was applied to the data sets simultaneously. The application of PCA resulted in no useful information as the features were too obstructed by background. However, comparison of the crater and magnetometry feature maps for the southern portion of the Pueblo site to the combined feature map, all shown in Figure 33, indicated that the features were not exactly spatially correlated. The incidence of cratering was most dense in the region between the two peaks of ordnance-related magnetic signal. Therefore, algorithms to quantify feature correlations from data subsequent to feature extraction will be developed in the second year of the project.

NRL outlined a tiered approach in the proposed data fusion framework for accomplishing data fusion, the principle task for year two of the program. Feature maps and their conversion to probability densities suitable for a Bayesian approach to data fusion were successfully obtained from the Pueblo PBR #2 survey data. These are a key enabling component for the data fusion framework.

First year efforts for project MM-1510 are summarized in Figure 33. Features relevant for wide area assessment of UXO contamination were successfully obtained from the various data sources. Taken individually, the results for each data source (expert information, orthophotography, LiDAR, and magnetometry) did not provide an accurate wide-area assessment of the Pueblo site. When the results were considered in tandem, for example, as shown combined feature map of Figure 33, the extracted features provided a more accurate wide-area assessment of the Pueblo site. For example, the crater-like

feature density map filled in the gap between the two peaks in the southern portion of the magnetometer signal density map. Thus, the target range known to be present in this area was used more extensively than indicated by historical sources. In addition, the density maps and the combined map all confirmed the presence of a second, but less used, target range located in the northern portion of the Pueblo site. No evidence in these maps supports the existence of the suspected 75 mm range. Ground truth dug in all three of these regions affirmed these conclusions, as shown in Figure 33.

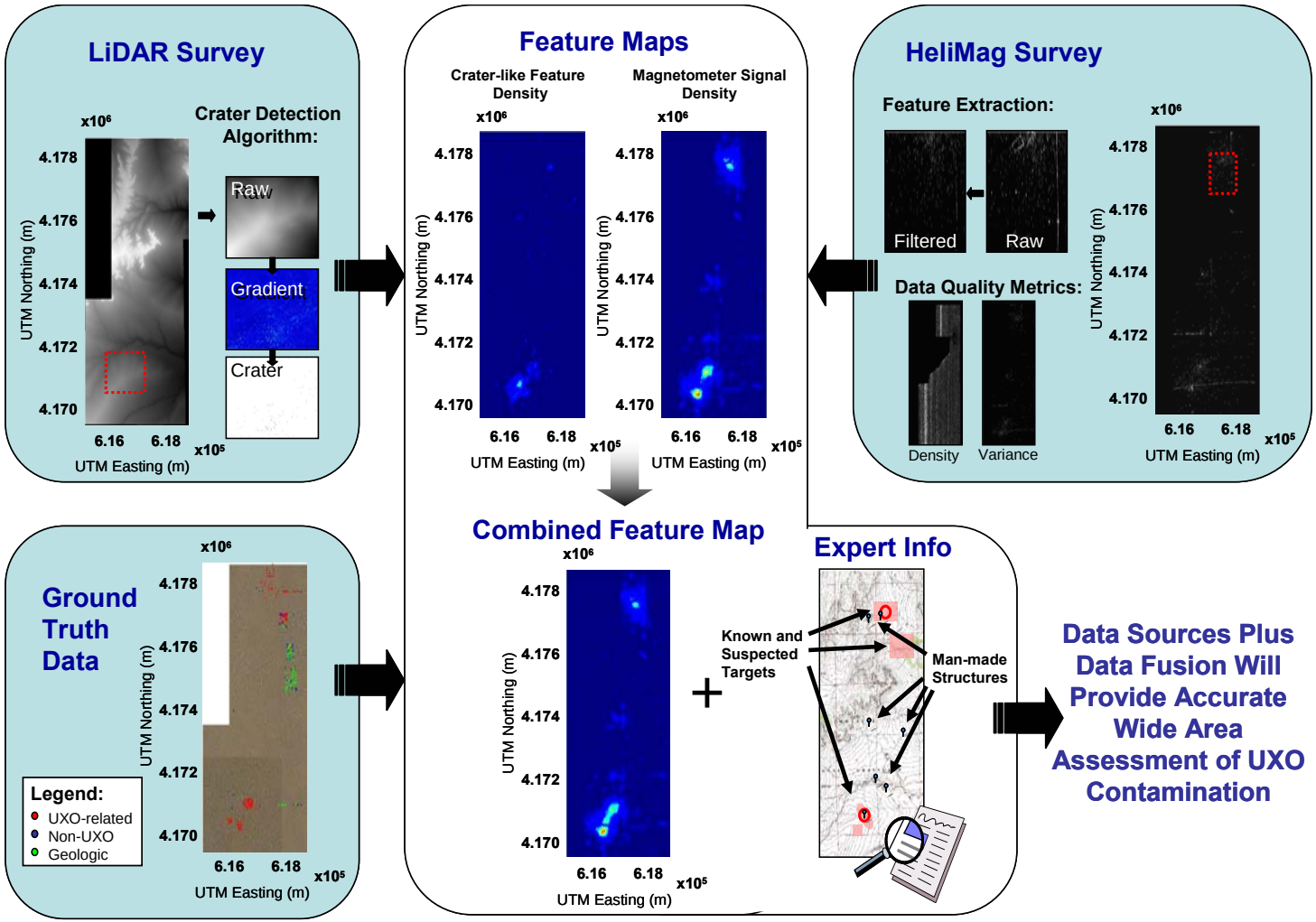

Figure 33 Summary of the first-year efforts of Project MM-1510

Summary

The first year of project MM-1510 successfully demonstrated the feasibility of feature extraction from wide-area assessment survey data. In contrast to the individual data sources, feature extraction yielded enhanced data for the Pueblo PBR #2 that was well-suited for data fusion. Preliminary combination of feature maps from the various data sources yielded a map for the Pueblo site that was more accurate than any one data source alone. Probability densities were generated from the feature maps and make possible the combination of estimates of data quality, UXO-related features, non-UXO backgrounds, and correlations among the data sets in a Bayesian-based approach to data fusion.

The feature extraction algorithms and the tiered approach to data fusion developed in the first year will enable a data fusion framework for wide area assessment to be an effective tool for UXO remediation of other sites. Although tailored to the specific data sources, the algorithms developed are general in nature and not overly site dependent. Large variations in the backgrounds for extracted features are expected for different remediation sites. However, these variations will most affect the signal-to-noise ratios in the maps for extracted features. The strength of a data fusion approach is that it provides resilience to such variations by maximizing the information obtained from the different data sources and minimizing exposure to false positives and background variations. The methods will provide a means to develop additional feature maps to quantify specific background features. Thus, the feature extraction algorithms and tiered approach to data fusion will be applicable to data sets from other survey sites. In summary, the results from the first year of project MM-1510 have only strengthened the case for the effectiveness of a data fusion approach for wide-area assessment.

References

1. Available at URLs <http://www.estcp.org/ux/#Wide> and <http://www.serdp.org/research/UXO.html>

2. Luo, R.C., Yih, C.C., Su, K.L., "Multisensor Fusion and Integration: Approaches, Applications, and Future Research Directions," *IEEE Sensors Journal* **2**(2) 107-119 (2002)

3. Luo, R.C., Su, K.L., "A Review of High-level Multisensor Fusion: Approaches and applications," *Proc. of IEEE Intl. Conf. on Multisensor Fusion and Integration for Intelligent Systems*, Taipei, Taiwan, R.O.C., Aug., 1999.

4. The Mathworks, Inc., "MATLAB Numerical Analysis Software Suite," at URL <http://www.mathworks.com>.

5. Duda, Richard O., Hart, Peter E., and Stork, David G. "Pattern Classification" John Wiley & Sons, New York, 2001.

6. "MexGDAL" was created by John Evans at Rutgers University and is available online via the Mathworks central file exchange. URL <http:/www.mathworks.com>

7. "GDAL" is an open-source translator library for raster geospatial data formats that is released under an X/MIT style Open Source license by the Open Source Geospatial Foundation and available freely online. URL <http://www.gdal.org>

8. US Army Corps of Engineers, "Archive Search Report, Findings: Pueblo PBR#2" Project B08CO071501, September, 1995.

9. SkyResearch Website, June 2006, URL <http:// gdc.skyresearch.com/ ESTCP_WAA/ photogallery/ Pueblo_Field/ index.htm>

10. Versar, Inc., "Conceptual site Models to Support ESTCP Wide Area Assessment Demonstration Project, Final Report," Springfield, VA , July 2005

11. Koenig, N.V., Scarbrough, A., TerBest, H., Garrison, R., "Evaluation of mineral and mineral fuel potential of Crowley and Otero Counties, state mineral lands administered by the Colorado State Land Board," *Electronic Resource CD*, Colorado Geological Survey, (2003)

12. Lupton, C.T. "Aerial and structural geologic map of Otero County, Colorado," Clason Map Company, 1926.

13. United States Department of Agriculture Soil Conservation Service, "Soil Survey of Otero County, Colorado," U.S. Government Printing Office, (1972)

14. Duce, J.T. "Geology of Parts of Las Animas, Otero and Bent Counties, Bulletin 27, Part III," Colorado Geological Survey, Boulder, CO, (1924)

15. Varshney, P.K.; Min Xu; Watanachaturaporn, P.; et al., "Decision tree regression for soft classification of remote sensing data," *Remote Sensing of Environment*, **97**(3), 322-36, (2005)

16. Mantero, P.; Moser, G.; Serpico, S.B., "Partially Supervised classification of remote sensing images through SVM-based probability density estimation," *IEEE Transactions on Geoscience and Remote Sensing*, **43**(3), 559-70, (2005)

17. Keuchel, J.; Naumann, S.; Heiler, M.; et al., "Automatic land cover analysis for Tenerife by supervised classification using remotely sensed data," *Remote Sensing of Environment*, **86**(4), 530-41, (2003)

18. Foody, G.M., "Fully fuzzy supervised classification of land cover from remotely sensed imagery with an artificial neural network," *Neural Computing & Applications* **5**(4), 238-47, (1997)

19. Cossu, R.; Chaudhuri, S.; Bruzzone, L., "A context-sensitive Bayesian technique for the partially supervised classification of multitemporal images," *IEEE Geoscience and Remote Sensing Letters*, **2**(3), 352-6, (2005)

20. Shrestha, R.L.; Carter, W.E.; Sartori, M.; et al., "Airborne Laser Swath Mapping: Quantifying changes in sandy beaches over time scales of weeks to years," *ISPRS Journal of Photogrammetry and Remote Sensing*, **59**(4), 222-32, (2005)

21. Rosso, P.H.; Ustin, S.L.; Hastings, A.' "Use of lidar to study changes associated with *Spartina* invasion in San Francisco Bay marshes," *Remote Sensing of Environment* **100**(3), 295-306, (2006)

22. Moffiet, T.; Mengersen, K.; Witte, C.; et al., "Airborne laser scanning: Exploratory data analysis indicates potential variables for classification of individual trees or forest stands according to species," *ISPRS Journal of Photogrammetry and Remote Sensing* **59**(5), 289-309, (2005)

23. Kimes, D.S.; Ranson, K.J.; Sun, G.; et al., "Predicting lidar measured forest vertical structure from multi-angle spectral data," *Remote Sensing of Environment* **100**(4), 503-11, (2006)

24. Streutker, D.R.; Glenn, N.F., "LiDAR measurement of sagebrush steppe vegetation heights," *Remote Sensing of Environment* **102**(1-2), 135-45, (2006)

25. Brock, J.C.; Wright, C.W.; Kuffner, I.B.; et al., "Airborne lidar sensing of massive stony coral colonies on patch reefs in the northern Florida reef tract," *Remote Sensing of Environment* **104**(1), 31-42, (2006)

26. Rivas, M.B.; Maslanik, J.A.; Sonntag, J.G.; et al., "Sea ice roughness from airborne LIDAR profiles," *IEEE Transactions on Geoscience and Remote Sensing* **44**(11), 3032-7, (2006)

27. Keqi Zhang; Jianhua Yan; Shu-Ching Chen, "Automatic construction of building footprints from airborne LIDAR data," *IEEE Transactions on Geoscience and Remote Sensing* **44**(9), 2523-33, (2006)

28. Sithole, G.; Vosselman, G., "Bridge detection in airborne laser scanner data," *ISPRS Journal of Photogrammetry and Remote Sensing* **61**(1), 33-46, (2006)

29. McLaughlin, R.A., "Extracting transmission lines from airborne LIDAR data," *IEEE Geoscience and Remote Sensing Letters* **3**(2), 222-6, (2006)

30. Forlani, G.; Nardinocchi, C.; Scaioni, M.; et al., "Complete classification of raw LIDAR data and 3D reconstruction of buildings," *Pattern Analysis and Applications* **8**(4) : 357-74, (2006)

31. Zhou, G.; Song, C.; Simmers, J.; et al., "Urban 3D GIS from LiDAR and digital aerial images," *Computers & Geosciences* **30**(4), 345-53, (2004)

32. Hong Wei; Bartels, M., "Unsupervised segmentation using Gabor wavelets and statistical features in LIDAR data analysis," *2006 18th International Conference on Pattern Recognition*, 20-24 Sept. 2006, Hong Kong, China

33. Silvan-Cardenas, J.L.; Wang, L., "A multi-resolution approach for filtering LiDAR altimetry data," *ISPRS Journal of Photogrammetry and Remote Sensing*, **61**(1), 11-22, (2006)

34. Bartels, M.; Hong Wei; MAson, D.C., "Wavelet packets and co-occurrence matrices for texture-based image segmentation," *Proceedings of Advanced Video and Signal based Surveillance (AVSS) 2005*, 15-16 Sept. 2005, Como, Italy, pg. 428-33

35. Wallace, J.; Morris, B.; Howarth, P., "The effects of scale on fractal dimension of topography: a case study from Sudbury, Ontario, Canada," *IGARSS 2004. 2004 IEEE International Geoscience and Remote Sensing*, 20-24 Sept. 2004, Anchorage, AK, USA, vol.5, pg. 2845-8

36. Zhang, Y., Collins, L.M., Yu, H., Baum, C.E., and Carin, L., "Sensing of Unexploded Ordnance with Magnetometer and Induction Data: Theory and Signal Processing" *IEEE Transactions on Geosciences and Remote Sensing*, **41**(5), 1005-1015, (2003)

37. Billings, S.D., "Discrimination and classification of buried unexploded ordnance using magnetometry," *IEEE Transactions on Geoscience and Remote Sensing*, **42**(6), 1241-51, (2004)

38. Hart, S.J., Shaffer, R.E. and Rose-Pehrsson, S.L., "Using Physics-Based Modeler Outputs to Train Probabilistic Neural networks for Unexploded Ordnance (UXO) Classification in Magnetometry Surveys," *IEEE Transactions on Geoscience and Remote Sensing*, **39**(4), 797 (2001)

39. Billings, S.D.; Pasion, C.; Walker, S.; et al., "Magnetic models of unexploded ordnance," *IEEE Transactions on Geoscience and Remote Sensing* **44**(8), 2115-24, (2006)

40. Barrow, B.; Nelson, H.H., "Model-based characterization of electromagnetic induction signatures obtained with the MTADS electromagnetic array," *IEEE Transactions on Geoscience and Remote Sensing* **39**(6), 1279-85, (2001)

41. Collins, L.M.; Yan Zhang; Jing Li; et al., "A comparison of the performance of statistical and fuzzy algorithms for unexploded ordnance detection," *IEEE Transactions on Fuzzy Systems* **9**(1), 17-30, (2001)

42. Collins, L.; Ping Gao; Schofield, D.; et al., "A statistical approach to landmine detection using broadband electromagnetic induction," *IEEE Transactions on Geoscience and Remote Sensing* **40**(4), 950-62, (2002)

43. Tobely, T.E.; Salem, A., "Position detection of unexploded ordnance from airborne magnetic anomaly data using 3-D self organized feature map," *2005 IEEE International Symposium on Signal Processing and Information Technology*, 18-21 Dec. 2005, Athens, Greece, pg. 322-7

44. Yan Zhang; Collins, L.M.; Carin, L., "Unexploded ordnance detection using Bayesian physics-based data fusion," *Integrated Computer-Aided Engineering* **10**(3), 231-47, (2003)

45. Collins, L.M.; Zhang, Y.; Carin, L., "Model-based statistical sensor fusion for unexploded ordnance detection," *Proceedings of IEEE International Geoscience and Remote Sensing Symposium. IGARSS 2002*, 24-28 June 2002, Toronto, Ont., Canada, vol. 3, pg. 1556-9

46. Rose-Pehrsson, S.L., Shaffer, R.E., McDonald, J.R., Grimm, R.E. and Lavely, E.M., "Annual Progress Report on Model-Based Data Fusion and Discrimination of UXO in Magnetometry and Electromagnetic," NRL/PU/6110--99-382 (1999)

47. Hu, W., Tantum, S.L., Collins, L.M., "EMI-Based Classification of Multiple Closely Spaced Subsurf Independent Components Analysis" *IEEE Transactions on Geosciences and Remote Sensing*, **42**(11), 2544-2554 (2004)

48. The "UX Detect" and "UX Process" modules for Oasis Montaj available online from Geosoft, Inc. at URL < http://www.geosoft.com/resources/tutorials/>

49. O'Neill, K.; Shubitidze, F.; Sun, K.; et al., "EMI obscuration of buried UXO by geophysical magnetic permeability, anthropogenic clutter, and by magnitude disparities," *Proceedings of the SPIE - The International Society for Optical Engineering* **5811**(1), 91-103, (2005)

50. Malinowski, E.R., "*Factor Analysis in Chemistry, Second Edition*," Wiley and Sons, New York, (1991)

51. Kimme, C., Ballard, D., Sklansky, J., "Finding Circles by an Array of Accumulators," *Comm. ACM*, **18**(2), 120-122, (1975)

52. The MATLAB script "CircularHough_Grd.m" was created by Tao Peng at the Univeristy of Maryland and is available online via the Matlab central file exchange at URL <http://www.mathworks.com/matlabcentral/>

53. Loy, G., Zelinsky, A., "Fast Radial Symmetry for Detecting Points of Interest," *IEEE Trans. Pattern Anal. and Machine Intell.*, **25**(8), 959-973, (2003)

54. Li Bai, Linlin Shen, Yan Wang, "A Novel Eye Location Algorithm based on Radial Symmetry Transform,"*Pattern Recognition,2006 18th Intnl. Conf. on Pattern Recog. (ICPR'06)*, **3**, 511-514, (2006)

55. Mallat, S.G., "A Theory for Multiresolution Signal Decomposition: The Wavelet Representation," *IEEE Transactions on Pattern Analysis and Machine Intelligence*, **11**, 674-693, (1989)

56. Mallat, S., "A Wavelet Tour of Signal Processing," Academic Press, San Diego, 1998.

57. Donoho, D.L. and Johnstone, I.M., "Threshold selection for wavelet shrinkage of noisy data," *Engineering in Medicine and Biology Society Annual International Conference of the IEEE*, (1994)

58. Donoho, D.L. and Coifman, R.L., "Translational-invariant de-noising," Technical report, Dept. of Statistics, Stanford University, (1995)

59. Duda, R.O., and Hart, P.E., "Use of the Hough transformation to detect lines and curves in pictures," *Communications of the ACM*, **15(1)**, 11-15 (1972)

Appendix A: Supporting Data

The common grid and feature maps are on contained in the attached DVD.

Appendix B: List of Technical Publications

Minor, C., Johnson, K. and Rose-Pehrsson, S., "Intelligent Data Fusion for Wide-Area Assessment of UXO Contamination," Partners in Environmental Technology Technical Symposium & Workshop, Washington, DC, November 28-30, 2006. (Poster)